



A positive feedback loop involving nuclear factor I β and calpain 1 suppresses glioblastoma cell migration

Received for publication, March 4, 2019, and in revised form, June 27, 2019. Published, Papers in Press, July 1, 2019, DOI 10.1074/jbc.RA119.008291

The Minh Vo, Saket Jain, Rebecca Burchett, Elizabeth A. Monckton, and Roseline Godbout¹

From the Cross Cancer Institute, Department of Oncology, University of Alberta, Edmonton, Alberta T6G 1Z2, Canada

Edited by Xiao-Fan Wang

Glioblastoma (GBM) is a brain tumor that remains largely incurable because of its highly-infiltrative properties. Nuclear factor I (NFI)-type transcription factors regulate genes associated with GBM cell migration and infiltration. We have previously shown that NFI activity depends on the NFI phosphorylation state and that calcineurin phosphatase dephosphorylates and activates NFI. Calcineurin is cleaved and activated by calpain proteases whose activity is, in turn, regulated by an endogenous inhibitor, calpastatin (CAST). The *CAST* gene is a target of NFI in GBM cells, with differentially phosphorylated NFIs regulating the levels of *CAST* transcript variants. Here, we uncovered an NFIB–calpain 1–positive feedback loop mediated through CAST and calcineurin. In NFI-hyperphosphorylated GBM cells, NFIB expression decreased the CAST–to–calpain 1 ratio in the cytoplasm. This reduced ratio increased autolysis and activity of cytoplasmic calpain 1. Conversely, in NFI-hypophosphorylated cells, NFIB expression induced differential subcellular compartmentalization of CAST and calpain 1, with CAST localizing primarily to the cytoplasm and calpain 1 to the nucleus. Overall, this altered compartmentalization increased nuclear calpain 1 activity. We also show that nuclear calpain 1, by cleaving and activating calcineurin, induces NFIB dephosphorylation. Of note, knockdown of calpain 1, NFIB, or both increased GBM cell migration and up-regulated the pro-migratory factors fatty acid-binding protein 7 (FABP7) and Ras homolog family member A (RHOA). In summary, our findings reveal bidirectional cross-talk between NFIB and calpain 1 in GBM cells. A physiological consequence of this positive feedback loop appears to be decreased GBM cell migration.

Glioblastomas (GBM),² classified as World Health Organization grade IV astrocytomas, are the most aggressive form of adult brain tumors (1). Despite recent advances in therapeutic intervention, the prognosis for GBM patients remains dismal,

with median survival times of ~15 months (2, 3). GBM cells are highly infiltrative, a property that may be driven by expression of neural stem markers. These stem-like/infiltrative properties allow GBM cells to evade conventional treatment, including surgery, chemotherapy (usually temozolomide), and radiation therapy (4–6). Without effective second-line treatment, patients often succumb to the disease shortly after tumor recurrence (7–9). Although significant effort has been made to unravel the mechanisms underlying GBM infiltration of normal brain tissue, we still have a poor understanding of what drives infiltration at the molecular level.

The nuclear factor I family of four transcription factors (NFIA, NFIB, NFIC, and NFIX) plays an integral role in regulating genes involved in neural cell migration and gliogenesis (10, 11). We have shown that NFIs regulate the neural progenitor/stem cell marker gene (brain fatty acid-binding protein, *FABP7*) (12, 13), whose expression is associated with higher GBM cell migration *in vitro* and infiltration *in vivo* (14–17). NFI regulation of *FABP7* depends on its phosphorylation state, with hypophosphorylated NFI up-regulating *FABP7* expression (12). NFIs are dephosphorylated by calcineurin phosphatase in GBM cells (18).

Calcineurin cleavage and activation are mediated by calpain, a family of calcium-dependent neutral proteases (19–21). The best-characterized calpains, calpain 1 (μ -calpain) and calpain 2 (m-calpain), are named based on the amount of calcium required for their activation *in vitro*: micro (μ)- or milli (m)-molar Ca^{2+} concentrations (21). Both calpains 1 and 2 function as heterodimers, composed of a distinct large subunit, CAPN1 (for μ -calpain) or CAPN2 (for m-calpain), and a shared smaller subunit (CAPSN1) (22). Calpain can either promote or inhibit cell migration depending on cell type. For example, inhibition of calpain 1 activity results in reduced platelet cell spreading (23). In contrast, inhibition of calpain 1 activity promotes random neutrophil migration (24). In addition, calpain 1 has been shown to prevent endothelial cell spreading as the result of calpain 1-mediated proteolysis of RhoA, a key factor in cell migration (25).

Calpain proteolytic activity is tightly regulated. Soon after its discovery, calpain was shown to undergo autolysis (or autolysis) (21). Autolyzed calpain requires lower calcium to reach half-maximal activity and thus is more active compared with full-length calpain (26). However, autolyzed calpain is also more unstable and prone to degradation and/or aggregation, the latter resulting in its inactivation (26). This instability may protect cells from detrimental effects associated with hyperac-

This work was supported by Canadian Institutes of Health Research Grant 130314. The authors declare that they have no conflicts of interest with the contents of this article.

¹ To whom correspondence should be addressed: Dept. of Oncology, University of Alberta, Cross Cancer Institute, 11560 University Ave., Edmonton, Alberta T6G 1Z2, Canada. Tel.: 780-432-8901; Fax: 780-432-8892; E-mail: rgodbout@ualberta.ca.

² The abbreviations used are: GBM, glioblastoma; NFI, nuclear factor I; FABP7, brain fatty acid-binding protein; NE, nuclear extract; CAST, calpastatin; CAPN, calpain; CnA, calcineurin; DAPI, 4',6-diamidino-2-phenylindole; FBS, fetal bovine serum; DMEM, Dulbecco's modified Eagle's medium; MTS, [3-(4,5-dimethylthiazol-2-yl)-5-(3-carboxymethoxyphenyl)-2-(4-sulfophenyl)-2H-tetrazolium, inner salt]; qPCR, quantitative PCR; ACM, aclinomycin A; LTP, long-term potentiation; PEI, polyethyleneimine.

NFIB–calpain 1-positive feedback loop in GBM cells

tive calpain. Calpain activity is also regulated by its highly-specific endogenous inhibitor, calpastatin (27). Binding of calpastatin to calpain not only inhibits its activity, but also prevents full autolysis of calpain leading to accumulation of the full-length form (28). Because calpastatin and calpain are ubiquitously expressed, their ratio and/or subcellular distributions may determine the level of calpain proteolytic activity within a cell.

Calpains can be inhibited by a wide array of exogenous inhibitors, including calpain inhibitor I (ALLN), a membrane-permeable synthetic peptide that specifically targets both calpain 1 and 2 *in vitro* (29). Aclacinomycin A (aclarcubicin, ACM), used for the treatment of patients with relapsed or refractory myeloid cancers, is a doxorubicin-like antibiotic that inhibits calpain activity (30–32).

We have previously shown that the *CAST* gene, encoding calpastatin, is a target of NFI in GBM cells. NFI functions through an alternative promoter containing two NFI-binding sites located in *CAST* intron 3 (33, 34). By differentially regulating the usage of *CAST* canonical and alternative promoters, NFI can alter the relative levels of *CAST* variants encoding full-length *versus* truncated calpastatin in GBM cells, with accompanying changes in the subcellular localization of calpastatin (33). NFI phosphorylation is an important determinant of *CAST* variant levels in GBM cells (33). Here, we show that NFIB regulation of *CAST* variants, and therefore calpastatin isoforms, affects calpain 1 levels and calpain 1 subcellular distribution in GBM cells. In turn, calpain 1 induces NFIB dephosphorylation through activation of calcineurin. This NFIB–calpain 1-positive feedback loop suppresses GBM cell migration but does not affect GBM cell survival.

Results

NFI directly regulates *CAST* but not calpain genes

We have previously shown that the expression of *CAST* variants in GBM cells depends on the NFI phosphorylation state (33). To examine how differentially-phosphorylated NFI affects calpastatin protein levels, we transiently transfected T98 (NFI-hyperphosphorylated) and U251 (NFI-hypophosphorylated) GBM cells (13) with either NFI expression constructs or previously validated siRNAs (12, 33, 34) targeting each of the four NFIs. Knocking down individual NFIs in NFI-hypophosphorylated U251 cells resulted in increased levels of calpastatin (Fig. 1A, left panel), with NFI overexpression having no effect on calpastatin (data not shown). In contrast, NFI depletion in NFI-hyperphosphorylated T98 GBM cells had no effect on calpastatin levels (data not shown). However, NFI overexpression reduced calpastatin levels (Fig. 1A, right panel). These data indicate that all four NFIs, through regulation of *CAST* variants, suppress the expression of calpastatin in GBM cells. Of note, the calpastatin antibody used for these experiments is specific to full-length calpastatin (~145 kDa), which has four calpain inhibitory domains (I–IV), the XL and the L N-terminal domains.

Calpastatin is an endogenous inhibitor of calpain. Because NFIs affect levels of calpastatin, we were interested in whether NFIs might also affect calpain activity through a calpastatin

feedforward loop. First, however, we wanted to ensure that NFI did not directly regulate calpain genes, as this would negate the need for a calpastatin-mediated feedforward loop. To address this possibility, we transiently transfected U87 and U251 GBM cells with siRNAs targeting each NFI member and carried out RT-qPCR using primers flanking the large subunit of calpain 1 (*CAPN1*), the large subunit of calpain 2 (*CAPN2*), and the small subunit (*CAPSNI*) that is shared by both calpains. Depletion of NFIs did not significantly affect *CAPN1*, *CAPN2*, and *CAPSNI* RNA levels (Fig. 1, B and C). Thus, NFI does not appear to regulate the transcription of calpain genes. In line with these results, we did not identify NFI-binding sites in the promoter regions of *CAPN1*, *CAPN2*, and *CAPSNI*, based on *in silico* analysis.

Differentially phosphorylated NFIB exert distinct effects on the subcellular distribution of calpain 1

Of the four NFIs, the role of NFIB in cancer is the best documented (35–37). Thus, we focused on examining the role of NFIB in the calpastatin/calpain pathway. To determine whether NFIB-mediated regulation of *CAST* affects calpains 1 and 2, we transiently transfected NFI-hyperphosphorylated U87 and NFI-hypophosphorylated U251 GBM cells (13) with two siRNAs targeting different regions of NFIB, and we carried out Western blot analysis using antibodies to either calpain 1 or calpain 2. Because calpain-mediated proteolysis of downstream effectors depends on the subcellular location of calpain, we carried out nuclear and cytoplasmic fractionation to investigate whether NFIB differentially affects calpain levels in these two cellular compartments.

Knocking down NFIB in U87 GBM cells had no effect on either the cytoplasmic or nuclear levels of calpain 2 (Fig. 2, A and B, left panels) but resulted in increased levels of full-length calpain 1 in the cytoplasm (Fig. 2A, left panel). Levels of calpain 1 in the nucleus were not affected (Fig. 2B, left panel). As depletion of NFIB in GBM cells increased overall levels of calpastatin (Fig. 1A), and calpastatin binds and inhibits calpain autolysis, our combined results suggest that hyperphosphorylated NFIB in U87 cells promotes activation of cytoplasmic calpain 1.

In contrast, depletion of NFIB in NFI-hypophosphorylated U251 cells had no effect on cytoplasmic calpain 1 (Fig. 2A, right panel) but led to a decrease in levels of an ~55-kDa autolyzed form of calpain 1 in the nucleus (Fig. 2B, right panel). Of note, we did not detect full-length calpain 1 in the nucleus of either U87 or U251 cells, suggesting that either autolysis of calpain 1 is required for its nuclear translocation or calpain 1 autolysis occurs with higher efficacy in the nucleus. These data suggest that hypophosphorylated NFIB can indirectly influence levels of nuclear, but not cytoplasmic, calpain 1. We used α -tubulin and lamin A/C as the loading controls for the cytoplasmic and nuclear fractions, respectively. NFIB knockdown efficiency is shown in both cell lines (Fig. 2C). Because NFIB depletion affected calpain 1, but not calpain 2, we focused on calpain 1 in subsequent experiments.

Next, we used immunostaining analysis to examine the effect of NFIB depletion on the subcellular distribution of calpastatin and calpain 1. In NFI-hyperphosphorylated U87 cells, calpastatin was found throughout the cytoplasm with little to no cal-

NFIB–calpain 1-positive feedback loop in GBM cells

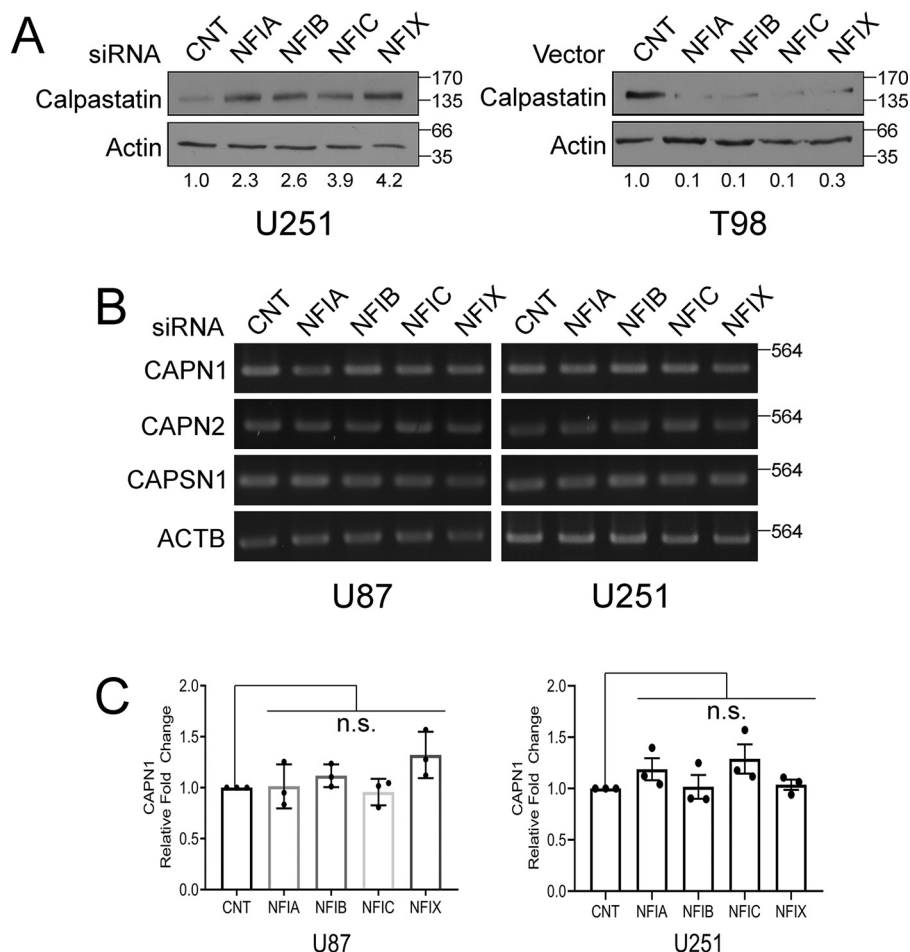


Figure 1. NFIB directly regulates *CAST* but not calpain genes. *A*, whole-cell lysates were prepared from T98 and U251 cells transfected with the indicated siRNAs (*left*) or NFI expression constructs (*right*). Proteins were separated by SDS-PAGE, electroblotted onto nitrocellulose membranes, and immunoblotted with a rabbit anti-calpastatin mAb or a mouse anti- β -actin antibody. Numbers below each lane represent fold changes in densitometric values relative to actin compared with control transfections ($n = 2$). *B* and *C*, U87 and U251 cells were transfected with siRNAs specific to each NFI member, and total RNA was extracted using the TRIzol reagent. *B*, cDNA was PCR-amplified using primers flanking the indicated genes, with actin serving as a loading control. *C*, cDNA was amplified by qPCR using *CAPN1*-specific primers. Relative fold changes were generated by normalizing *CAPN1* data to those of *GAPDH* and then to the internal scrambled siRNA control. Results are representative of three independent experiments. *n.s.*, p value > 0.05 .

pastatin in the nucleus. NFIB depletion resulted in increased aggregation of calpastatin surrounding the nucleus, with no apparent effect on nuclear calpastatin (Fig. 3*A*, arrow). These two patterns of localization have been reported for calpastatin in other systems (38, 39). Similarly, NFIB depletion in U87 cells resulted in increased cytoplasmic aggregation of calpain 1 to one side of the cell (see arrow, Fig. 3, *A* and *C*, left panel). These observations suggest an association between hyperphosphorylated NFIB and disaggregation of cytoplasmic calpastatin and calpain 1.

We have previously shown that calpastatin has a perinuclear distribution in NFI-hypophosphorylated U251 cells, with NFIB depletion resulting in increased levels of nuclear calpastatin (33). Here, we show that calpain 1 is primarily in the nucleus of U251 cells (Fig. 3*B*). NFIB knockdown resulted in decreased levels of nuclear calpain 1 (Fig. 3*C*, right panel), presumably the autolyzed form of calpain 1 based on our Western blottings (Fig. 3*B*). These results point to a role for hypophosphorylated NFIB in the differential localization of calpastatin (to the cytoplasm) and calpain 1 (to the nucleus).

NFIB depletion decreases calpain activity and GBM cell migration but does not affect GBM cell viability

Whether through accumulation of cytoplasmic full-length calpain 1 (as observed in NFI-hyperphosphorylated U87 cells) or loss of autolyzed nuclear calpain 1 (as observed in NFI-hypophosphorylated U251 cells), our results, taken in light of evidence from the literature, point to reduced calpain 1 activity upon NFIB depletion in GBM cells. To investigate how calpain 1 proteolytic activity changes upon NFIB depletion, we transiently transfected U87 and U251 cells with two siRNAs targeting NFIB and then measured calpain activity using a fluorometric substrate. NFIB depletion resulted in decreased calpain proteolytic activity in both cell lines. Specifically, NFIB knockdown in U87 cells resulted in lower levels of relative fluorescence intensity, to 0.29-fold (siNFIB-1, $p < 0.0001$) and 0.55-fold (siNFIB-2, $p < 0.001$), compared with scrambled siRNA-transfected cells (Fig. 4*A*, left panel). Similarly, NFIB depletion in U251 cells resulted in reduced levels of relative fluorescence intensity, to 0.51-fold (siNFIB-1, $p < 0.0001$) and 0.57-fold (siNFIB-2, $p < 0.001$), compared with scrambled

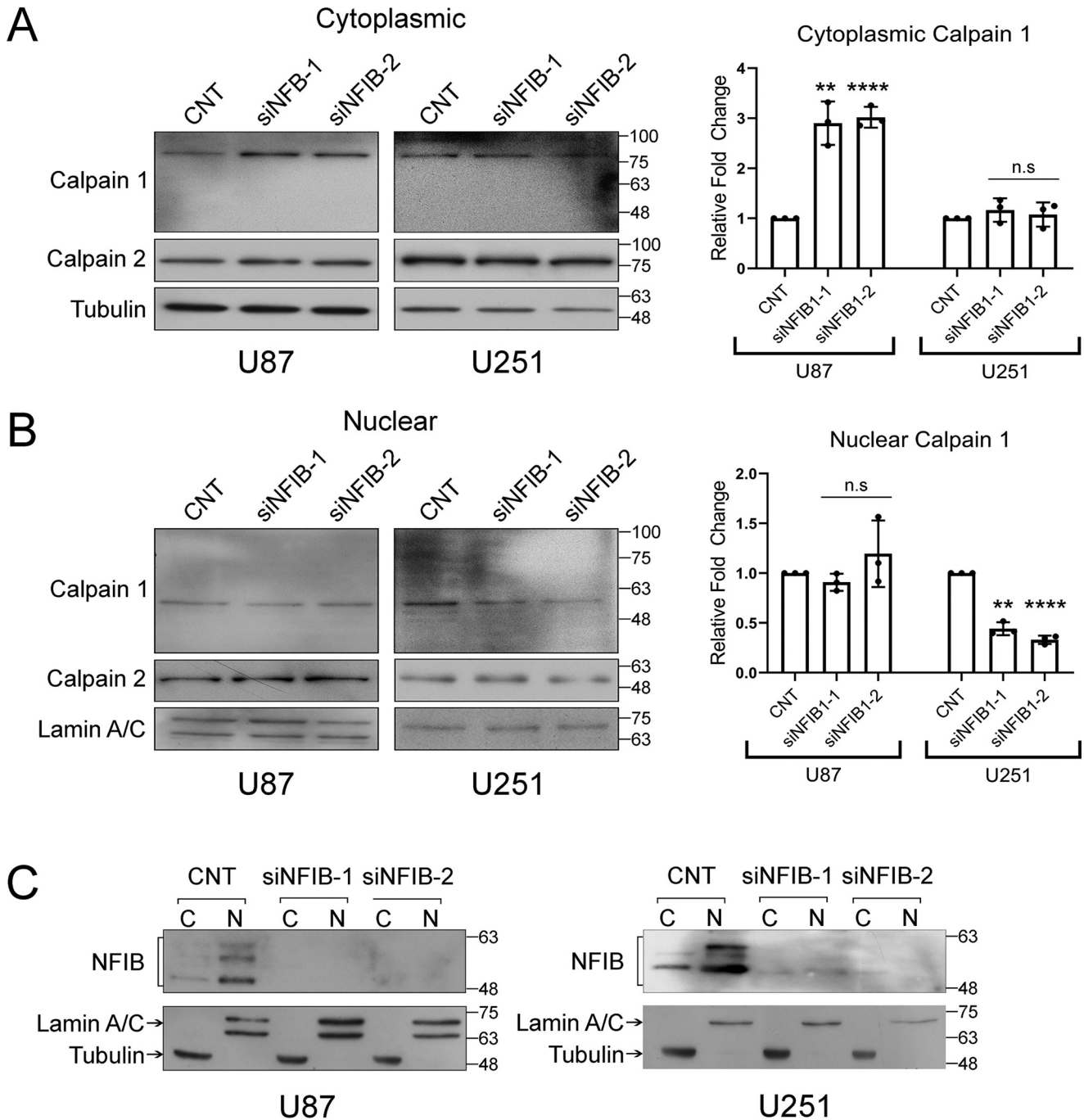


Figure 2. Changes in cytoplasmic and nuclear calpain 1 levels upon NFIB knockdown. U87 and U251 cells were transfected with scrambled (control, CNT) siRNAs or two different siRNAs targeting NFIB. Cytoplasmic (A), nuclear (B), or both cytoplasmic and nuclear (C) lysates were prepared using the NE-PER kit, electrophoresed on polyacrylamide gel, and transferred to nitrocellulose membranes. Blots were immunostained with mouse anti-calpain 1 and rabbit anti-calpain 2 antibodies. α -Tubulin and lamin A/C served as loading controls for the cytoplasmic and nuclear fractions, respectively. Histograms represent relative fold changes in densitometric values compared with scrambled siRNA control ($n = 3$) (n.s., p value >0.05 ; **, p value <0.01 ; and ****, p value <0.0001). C, blots are representative of three independent experiments. Abbreviations used are as follows: C, cytoplasmic; N, nuclear.

siRNA-transfected cells (Fig. 4A, right panel). Whereas our calpain activity fluorometric assay does not differentiate between calpain 1 and calpain 2, our Western blottings show that calpain 2 levels are not affected by NFIB knockdown (Fig. 2, A and B). As NFIB depletion reduced total calpain activity to $\sim 50\%$ compared with control cells, we conclude that the effect of NFIB on calpain activity is mediated chiefly through calpain 1.

We used the Transwell assay to examine how reduced calpain 1 proteolytic activity in NFIB-depleted cells affects GBM

cell migration. NFIB knockdown in U87 and U251 cells resulted in ~ 3 - and ~ 2 -fold increases in numbers of migrating cells, respectively (Fig. 4B). Specifically, the number of migrated U87 cells increased from 392 to 1179 in control- versus siNFIB-1-treated cells (~ 3 -fold, $p < 0.0001$). Likewise, the number of migrated U251 cells increased from 433 to 843 in control- versus siNFIB-1-treated cells (~ 2 -fold, $p < 0.0001$). These results suggest that NFIB inhibits GBM cell migration, irrespective of the NFI phosphorylation state.

NFIB–calpain 1-positive feedback loop in GBM cells

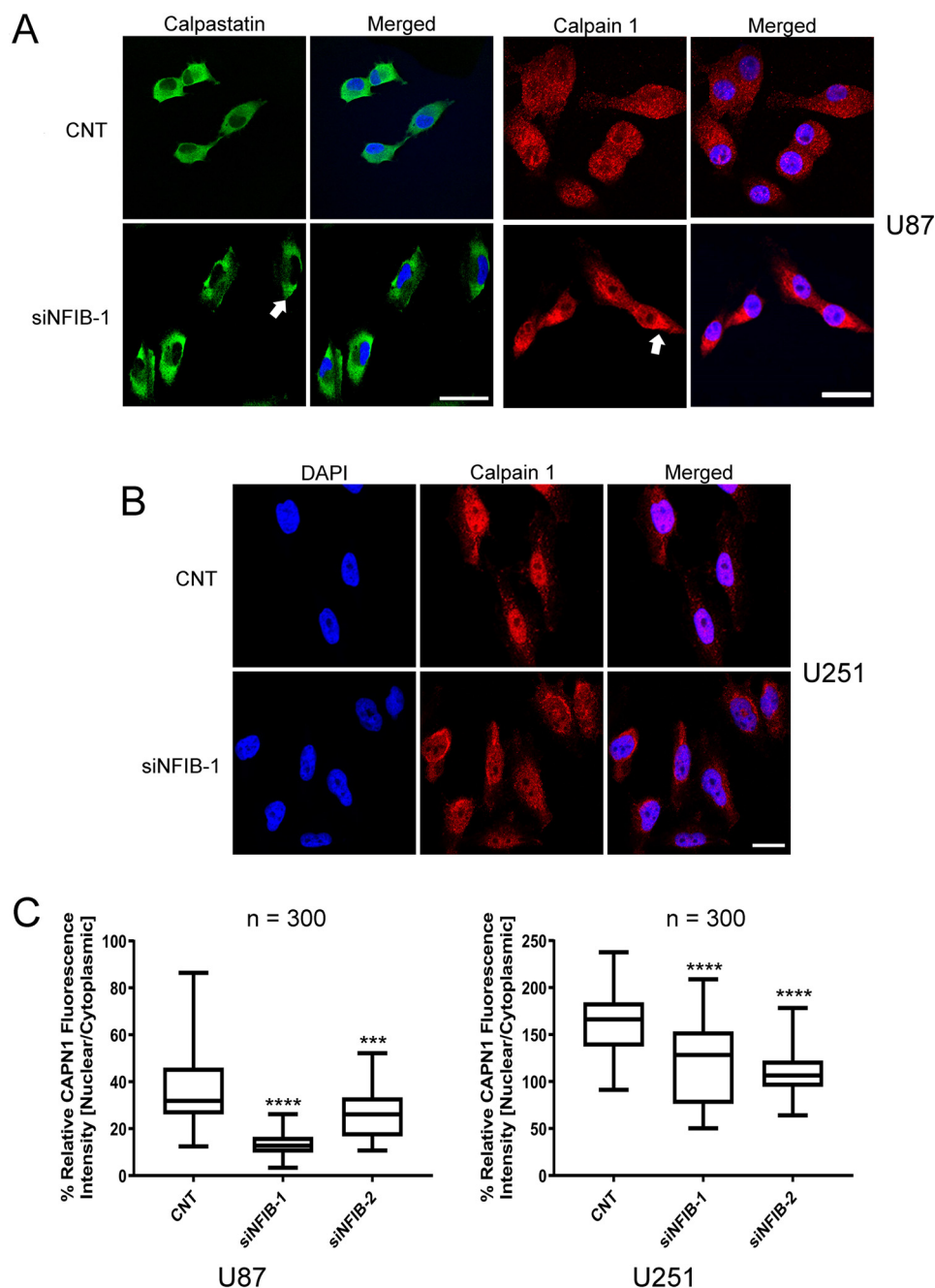


Figure 3. Changes in calpastatin and calpain 1 subcellular localization upon NFIB depletion. U87 (A) or U251 (B) cells were transiently transfected with scrambled (control, *CNT*) siRNAs or an NFIB-specific siRNA and then plated onto coverslips. Cells were cultured for 24 h and then fixed with 4% paraformaldehyde and immunostained with either rabbit anti-calpastatin (A) or mouse anti-calpain 1 (A and B) antibodies followed by Alexa 488 (rabbit, *green*)- or Alexa 555 (mouse, *red*)-conjugated secondary antibodies, respectively. Nuclei were visualized with DAPI (*blue*), and images were acquired with a $\times 40/1.3$ oil immersion lens using the Zeiss LSM 710 confocal microscope and Zeiss ZEN imaging software. Bars, 20 μm . Images are representative of the majority of cells observed under each condition and are derived from three independent experiments. C, for quantification of calpain 1 subcellular localization, fluorescence intensity values in the *red* channel (calpain 1) were generated for nuclear (DAPI as marker) and cytoplasmic fractions using 300 random U251 cells (100 cells for each biological replicate). Data are presented as percent nuclear fluorescence intensity relative to cytoplasmic fluorescence intensity. (***, p value < 0.001 , and ****, p value < 0.0001 .)

We also examined the effect of NFIB depletion on GBM cell survival using the MTS assay. The MTS assay measures cell metabolism and is a surrogate assay for cell viability (40). NFIB knockdown had no effect on cell viability in both U87 ($p > 0.65$) and U251 ($p > 0.48$) cells (Fig. 4C). These observations indicate that NFIB–calpastatin–calpain 1 cross-talk may not be important for GBM cell viability.

Calpain 1 depletion induces NFIB phosphorylation

So far, we have shown that NFIB affects calpain 1 levels and activity, with concomitant changes in levels and subcellular distribution of calpastatin. Here, we address the possibility of bidirectional signaling between calcineurin/NFIB and calpain 1 in GBM cells. We transiently transfected NFIB-hypophosphorylated U251 cells with two siRNAs targeting calpain 1 and exam-

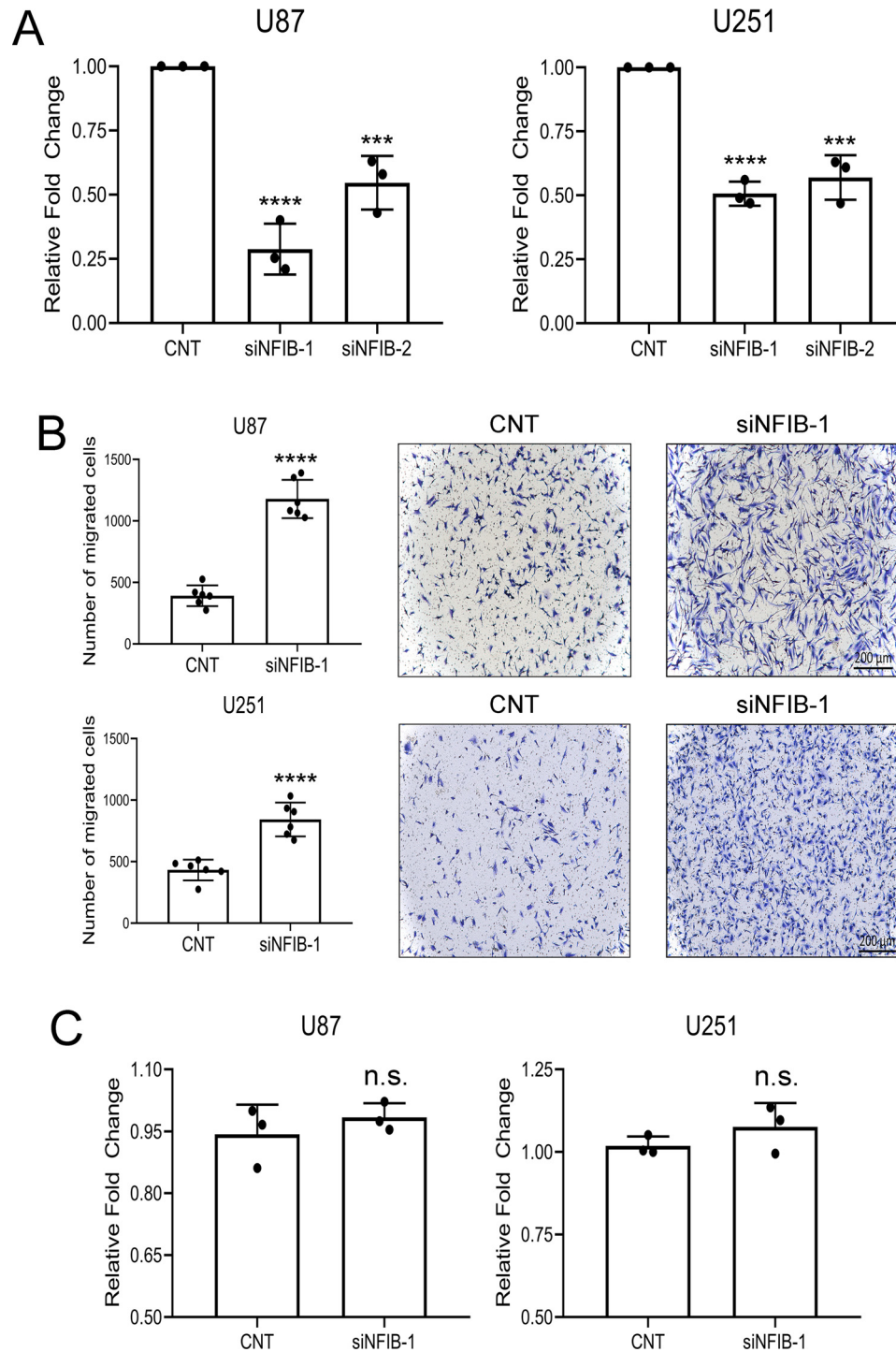


Figure 4. Effects of NFIB depletion on calpain activity and GBM cell migration and viability. A–C, U87 and U251 cells were transfected with scrambled siRNAs or siRNAs targeting NFIB. A, calpain activity was assessed by measuring the cleavage of a synthetic substrate provided in the calpain activity fluorometric assay kit (Calbiochem). Fluorescent signals obtained in a buffer that activates calpain activity was normalized against fluorescent signals obtained in a buffer that inhibits calpain activity. Relative fold change was obtained by normalizing the scrambled siRNA control to 1. B, 30,000 cells in FBS-free DMEM were seeded in the top chambers of Falcon cell culture inserts in a 24-well plate. Directional migration was induced by supplementing the medium in the bottom chamber with 10% FBS. After 20 h, cells that had migrated through the porous membrane of the inserts were fixed with methanol and stained with crystal violet. Migrated cells were imaged with the Zeiss Axioskop2 plus microscope. Cells were counted using MetaMorph software. Bars, 200 μ m. C, cell metabolism, used as a surrogate for cell viability, was measured using the MTS assay. 3500 cells were seeded in 96-well plates. After 48 h, cells were incubated with the MTS reagent for 2 h. Fluorescence emission (495 nm) was measured using the FLUOstar Optima plate reader and then normalized to the scrambled siRNA control. Each experiment was repeated at least three times. (n.s., p value >0.05 ; ***, p value <0.001 , and ****, p value <0.0001).

ined the effect of calpain 1 depletion on the catalytic subunit of calcineurin and NFIB phosphorylation. In keeping with calcineurin being cleaved and activated by calpain 1 (19, 20),

knocking down calpain 1 resulted in accumulation of the uncleaved form of calcineurin (~60 kDa) in the cytoplasm of U251 cells (Fig. 5A). Loss of calpain 1 also led to increased levels

NFIB–calpain 1-positive feedback loop in GBM cells

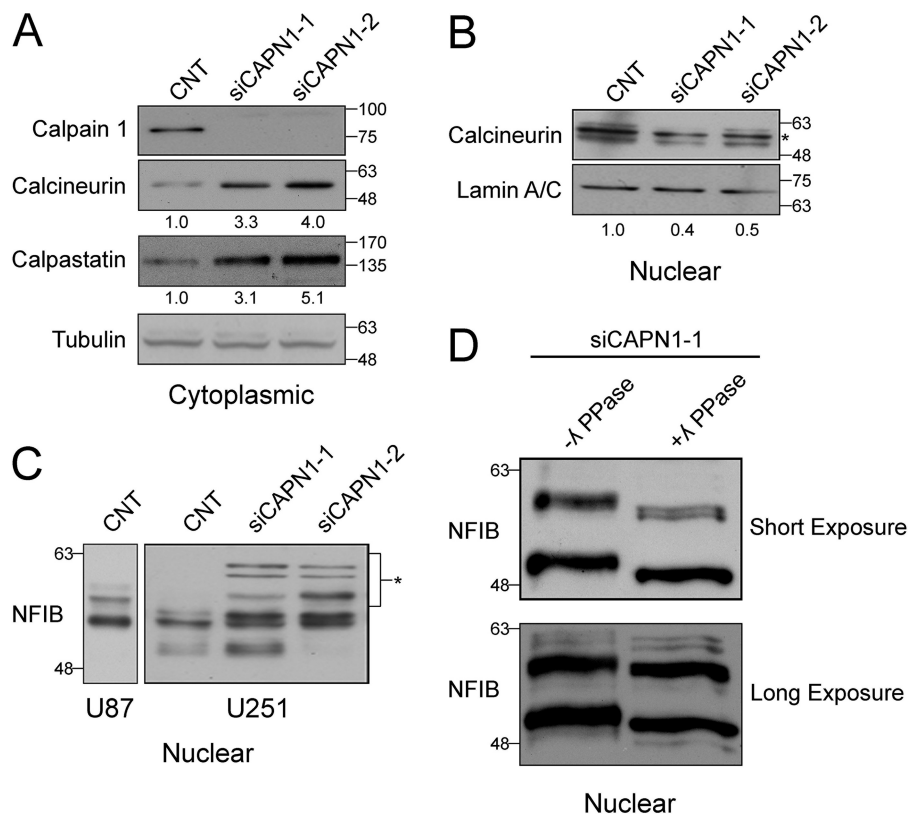


Figure 5. Calpain 1 depletion affects levels of calpastatin and calcineurin as well as NFIB dephosphorylation. Cytoplasmic (A) and nuclear lysates (B) were prepared from U251 cells transiently transfected with scrambled siRNAs or siRNAs targeting calpain 1 (*siCAPN1-1* and *siCAPN1-2*). Numbers represent relative fold changes in densitometric values compared with control transfections ($n = 2$). The asterisk indicates the cleaved form of calcineurin. C, nuclear fractions were prepared from U87 and U251 cells transfected with scrambled siRNAs (CNT) or siRNAs targeting calpain 1 (*siCAPN1-1* and *siCAPN1-2*). Blots are representative of three independent experiments. The asterisk indicates the hyperphosphorylated forms of NFIB. D, nuclear extracts were prepared from U251 cells transfected with CAPN1-1 siRNA in the absence of phosphatase inhibitors and then treated with λ -phosphatase (λ PPase) for 1 h at 30 °C. Blots are representative of two independent experiments. A–D, proteins were electrophoresed on SDS-polyacrylamide gels and transferred to nitrocellulose membranes. Blots were immunostained with mouse anti-calpain 1, mouse anti-calcineurin, rabbit anti-calpastatin, and rabbit anti-NFIB antibodies. α -Tubulin and lamin A/C were used as loading controls for cytoplasmic and nuclear fractions, respectively.

of full-length calpastatin in U251 cells (Fig. 5A), which agrees with our previous findings showing that NFI-hyperphosphorylated GBM cells preferentially express full-length calpastatin (33).

As expected, depletion of calpain 1 also resulted in decreased levels of the cleaved forms of calcineurin in U251 cells (Fig. 5B; indicated by the asterisk). Of note, cleaved calcineurin was only observed in the nucleus of U251 cells, suggesting that the cleavage of calcineurin occurs after its nuclear translocation and thus can be influenced by calpain 1 concentration in the nucleus. This observation may explain how NFI remains hyperphosphorylated in U87 cells despite increased cytoplasmic calpain 1 levels. Along with reduced calcineurin cleavage, we observed hyperphosphorylation of NFIB in calpain 1-depleted U251 cells compared with control cells (asterisk in Fig. 5C). It is noteworthy that these hyperphosphorylated forms of NFIB migrate even more slowly than those observed in U87 cells (Fig. 5C), suggesting that NFIB exists in a basally hyperphosphorylated state in control (*i.e.* noncalpain 1-depleted) U87 GBM cells. To confirm that the slower-migrating forms of NFIB observed upon calpain 1 depletion are indeed hyperphosphorylated, we treated U251 cell extracts with λ -phosphatase. All the NFIB bands underwent a reduction in size after λ -phosphatase treatment (Fig. 5D). Of note, the banding patterns of

NFIB were different depending on whether phosphatase inhibitors were included (Fig. 5C) or not (Fig. 5D). This is likely due to the potent phosphatase activity of calcineurin, which may dephosphorylate NFIB in the absence of phosphatase inhibitors. Together, our data support the second signaling branch of the NFIB–calpain 1 cross-talk in GBM cells; calpain 1 cleaves and activates calcineurin, which in turn dephosphorylates NFIB in U251 cells.

Calpain 1 depletion alters the subcellular distribution of calcineurin and NFIB

We performed immunofluorescence analysis of calpain 1-depleted U251 (NFI-hypophosphorylated) cells to further investigate the effect of calpain 1 on the subcellular localization of calcineurin and NFIB. In control cells, both NFIB and calcineurin had a diffuse nuclear pattern (Fig. 6A, 1st row). Calpain 1 knockdown resulted in reduced levels of calcineurin in the nucleus with much higher levels of calcineurin in the cytoplasm (Fig. 6, A, 2nd row, and B, right panel). These results are in agreement with our Western blotting data (Fig. 5A). Loss of calpain 1 also led to changes in the immunostaining pattern of NFIB such that NFIB appeared to be excluded from nucleoli compared with control cells (Fig. 6, A, 2nd row, and B, left panel).

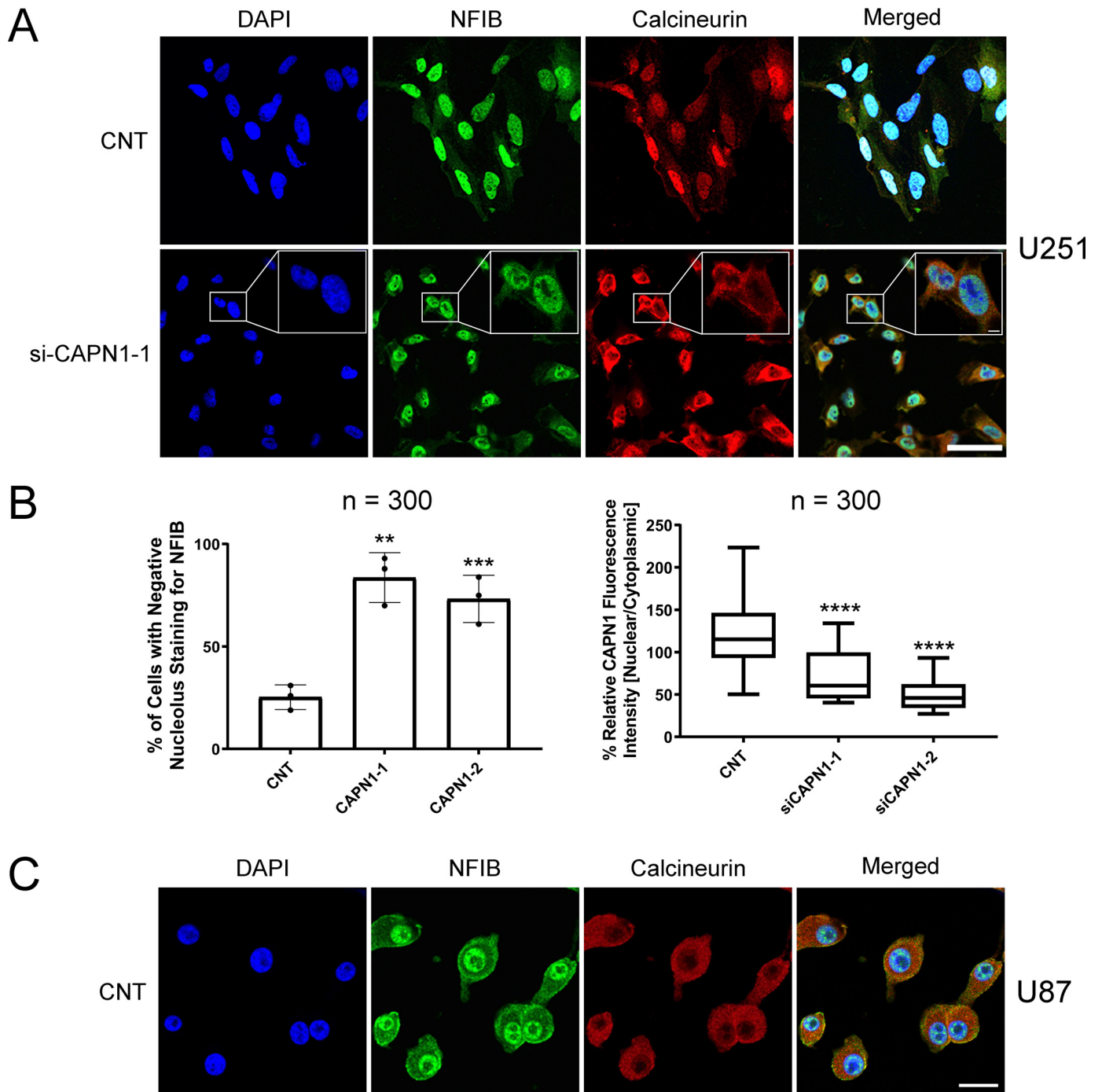


Figure 6. Changes in calcineurin and NFIB subcellular localization upon calpain 1 depletion. U251 (A and B) or U87 (C) cells were transiently transfected with scrambled siRNAs or calpain 1-specific siRNAs and then plated on coverslips. Cells were cultured for 24 h and then fixed with 4% paraformaldehyde and immunostained with rabbit anti-NFIB and mouse anti-calcineurin antibodies followed by Alexa 488 rabbit (green)- or Alexa 555 mouse (red)-conjugated secondary antibodies, respectively. Nuclei were visualized with DAPI (blue), and images were acquired with a $\times 40/1.3$ oil immersion lens using the Zeiss LSM 710 confocal microscope and Zeiss ZEN imaging software. Bars, 50 μm (A) and 5 μm (insets); 20 μm (C). Images are representative of the majority of cells observed under each condition and are derived from three independent experiments. B, 300 random U251 cells (100 cells for each biological replicate) were used for NFIB and calcineurin quantification. For NFIB nucleolus localization, cells showing absence of nucleolar staining in the green channel (NFIB) were manually counted. Data are presented as percent of cells negative for nucleolar NFIB immunostaining relative to total number of cells counted. For calcineurin subcellular localization, fluorescence intensity values in the red channel (calcineurin) were generated for nuclear (DAPI as marker) and cytoplasmic fractions. Data are presented as percent nuclear fluorescence intensity relative to cytoplasmic fluorescence intensity. (**, p value < 0.01 ; ***, p value < 0.001 , and ****, p value < 0.0001).

It is noteworthy that the subcellular distribution of calcineurin and NFIB in calpain 1-depleted U251 cells was similar to that observed in control U87 (NFI-hyperphosphorylated) cells (Fig. 6C). These observations suggest that the phosphorylation

state of NFIB may influence its subcellular distribution. Thus, calpain 1 may alter NFIB subcellular localization through modulation of calcineurin phosphatase activity. Taken together, our data support a positive feedback loop between NFIB and cal-

NFIB–calpain 1-positive feedback loop in GBM cells

calpain 1 such that NFIB, through calpastatin, promotes autolysis and activation of calpain 1. In turn, calpain 1 up-regulates calcineurin phosphatase activity, which results in NFIB dephosphorylation, which has been previously correlated with increased transcriptional activity (12, 13, 18).

Calpain 1 depletion increases GBM cell migration but does not affect cell survival

To understand the effects of the NFIB–calpain 1-positive feedback loop on GBM cell migration and cell survival, we repeated the Transwell assay using U87 and U251 cells depleted of either calpain 1 or both calpain 1 and NFIB. Similar to NFIB depletion, knocking down calpain 1 resulted in increased cell migration in both cell lines. Specifically, the number of migrated cells increased from 392 in control to 917 in siCAPN1-transfected U87 cells (~2.34-fold increase, $p < 0.0001$) (Fig. 7A). Likewise, the number of migrated cells increased from 433 in control to 991 in siCAPN1-transfected U251 cells (~2.29-fold, $p < 0.0001$) (Fig. 7B). These data indicate that calpain 1, like NFIB, inhibits GBM cell migration. Co-depletion of NFIB and calpain 1 in U87 cells led to a statistically significant further increase in the number of migrated cells compared with calpain 1 depletion: 1238 cells for the former versus 917 cells for the latter (~1.35-fold, $p < 0.01$) (Fig. 7A). Similar results were obtained with U251 cells: 1965 cells for NFIB/calpain 1 co-depletion compared with 991 cells for calpain 1 depletion alone (~1.98-fold, $p < 0.001$) (Fig. 7B). In agreement with our proposed role for NFIB in the negative regulation of GBM cell migration, NFIB ectopic expression resulted in decreased numbers of migrated cells compared with control (~0.23-fold, $p < 0.0001$, Fig. 7C). Importantly, co-transfection of U251 cells with both a calpain 1-specific siRNA and an NFIB expression construct reversed the NFIB-induced reduction in cell migration observed in NFIB-overexpressing U251 cells ($p < 0.01$, Fig. 7C). These data indicate that the negative effect of NFIB on GBM cell migration is at least partly mediated through calpain 1 signaling, thereby providing functional support for our proposed NFIB–calpain 1-positive feedback loop.

Similar to NFIB knockdown, depletion of either calpain 1 or both NFIB and calpain 1 had no effect on either U87 ($p > 0.32$ and $p > 0.74$, respectively) or U251 ($p > 0.18$ and $p > 0.85$, respectively) cell survival as measured by the MTS assay (Fig. 7F). Our data thus indicate that NFIB and calpain 1 act in concert to dampen GBM cell migration but have no effect on cell proliferation. However, given the further increases in cell migration observed upon co-depletion of calpain 1 and NFIB compared with calpain 1-depleted GBM cells (Fig. 7, A and B), NFIB and calpain 1 may have target genes and downstream effectors that are independent from NFIB–calpain cross-talk.

Calpain 1 depletion increases levels of RhoA and FABP7, both implicated in GBM cell migration

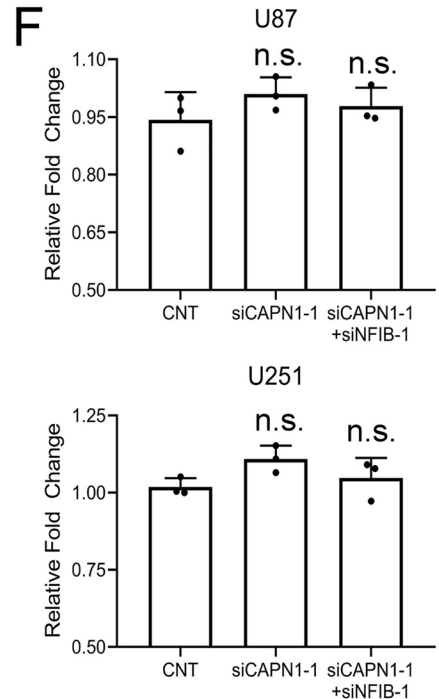
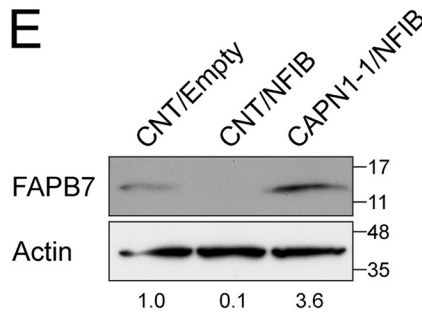
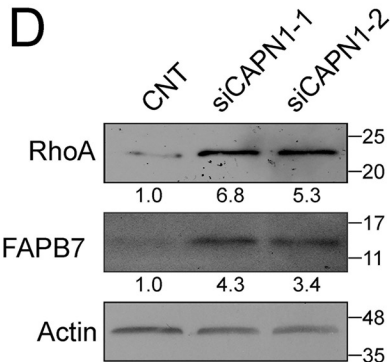
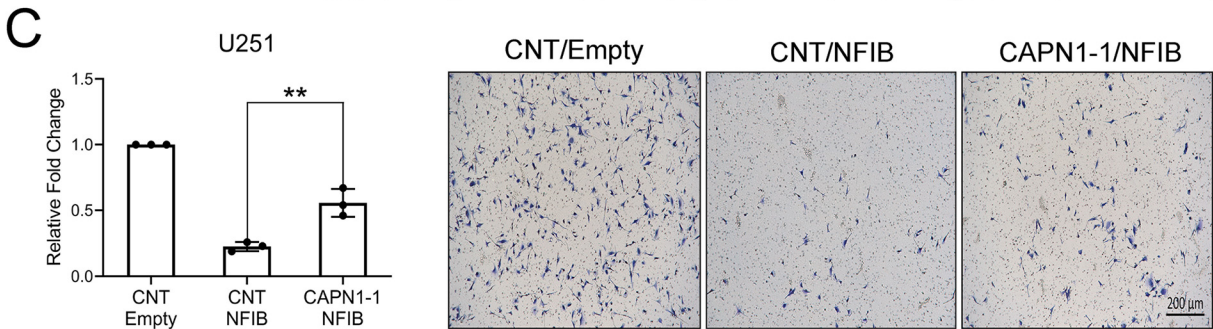
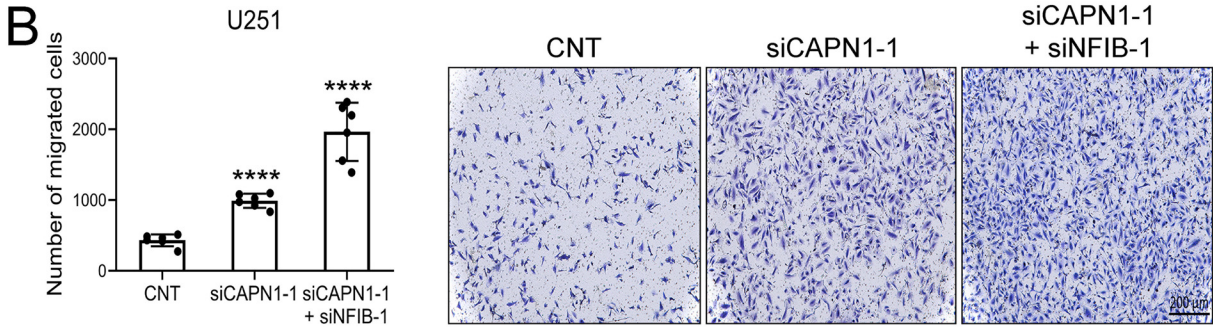
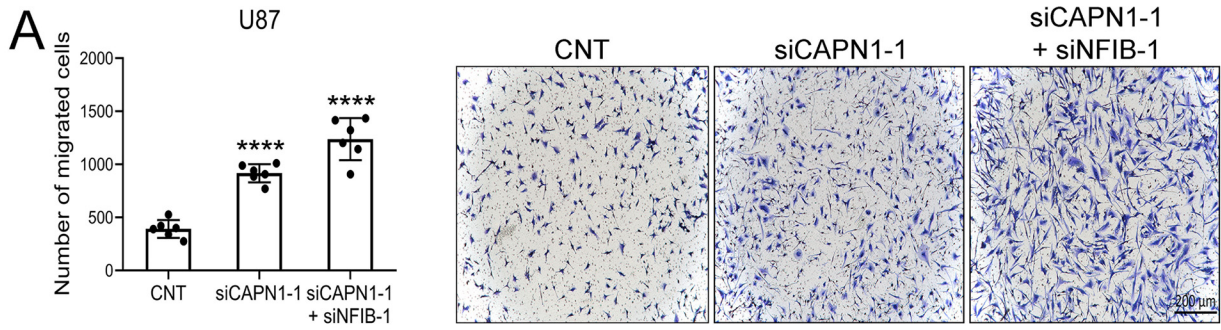
To gain mechanistic insights into calpain 1's role in the inhibition of GBM cell migration, we examined the levels of the pro-migratory factor RhoA. Cleavage of RhoA by calpain 1 has previously been shown to reduce spreading in bovine aortic endothelial cells (25). Calpain 1-depleted U251 cells showed a

5–7-fold increase in uncleaved RhoA (22 kDa) compared with control cells (Fig. 7D). These results are in line with RhoA serving as an important regulator of GBM cell migration (41, 42). Although our antibody did not detect cleaved RhoA (20 kDa), perhaps due to the labile nature of this truncated form, our results are consistent with calpain 1-mediated proteolysis of RhoA being a downstream mechanism by which the NFIB–calpain 1 feedback loop down-regulates GBM cell migration.

Brain fatty acid-binding protein (FABP7) is a target of NFI transcription factors that has been directly linked to increased GBM cell migration (12, 13, 17, 43). To examine whether the NFIB–calpain 1 cross-talk exerts its negative regulation on GBM cell migration through FABP7, we transfected U251 cells with calpain 1 siRNAs. Calpain 1 depletion led to a 3–4-fold increase in levels of FABP7 (Fig. 7D). Next, we ectopically expressed NFIB in U251 cells. A consistent decrease in FABP7 protein levels was observed in these cells compared with control cells (Fig. 7E). Finally, by transfecting NFIB-overexpressing U251 cells with calpain 1 siRNAs, we showed recovery of FABP7 protein levels to that observed in control cells (Fig. 7E). The parallels in the effects NFIB and calpain 1 have on FABP7 expression and GBM cell migration (Fig. 7C), combined with FABP7's previously demonstrated pro-migratory effects, suggest a central role for our proposed NFIB–calpain 1-positive feedback loop on regulating GBM cell migration through FABP7.

Targeting the NFI–calpain pathway in GBM cells using calpain inhibitors

It is well-known that calpains 1 and 2 can functionally compensate for the loss of one another under certain conditions, including the cleavage and activation of calcineurin (19, 20). To bypass this compensatory pathway, we examined the effect of two inhibitors targeting both calpains 1 and 2, ACM and ALLN, on GBM cell viability using the colony formation assay. Both T98 (NFI-hyperphosphorylated) and U251 (NFI-hypophosphorylated) cells showed a dose-dependent decrease in colony formation in response to either ACM or ALLN treatment (Fig. 8A). The LD₅₀ values for ACM and ALLN were ~10 nM and ~10 μM, respectively (Fig. 8A). At higher doses of ACM (100 nM) and ALLN (10 μM), we observed a significant difference between T98 (NFI-hyperphosphorylated) and U251 (NFI-hypophosphorylated) colony formation, with 10.4% of plated T98 cells forming colonies compared with 1% of plated U251 cells in the case of ACM ($p < 0.0001$) and 18.8% of plated T98 cells forming colonies compared with 11.4% of plated U251 cells in the case of ALLN ($p < 0.0001$) (Fig. 8A). We also observed differences in cell viability that were dependent on the NFI-phosphorylation state of U87 (NFI-hyperphosphorylated) and U373 (NFI-hypophosphorylated) (13) GBM cells at the higher ACM doses using the MTS assay (Fig. 8B). Together, these results suggest the following: (i) inhibition of combined calpain 1 and 2 activity reduces GBM cell survival/proliferation, and (ii) GBM cells with hyperphosphorylated NFI may be more resistant to calpain inhibitors than GBM cells with hypophosphorylated NFI.



NFIB–calpain 1-positive feedback loop in GBM cells

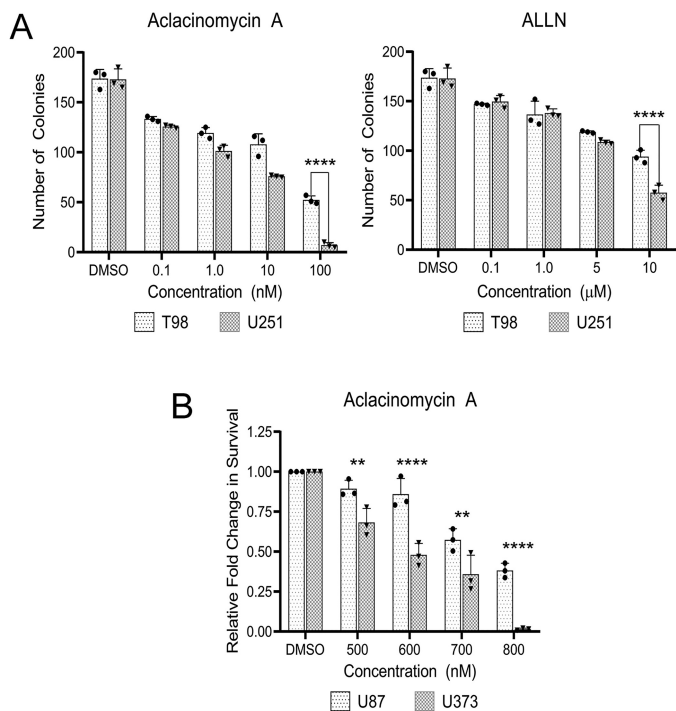


Figure 8. Effects of calpain inhibitors on GBM cell clonogenic survival. *A*, 500 T98 (NFI-hyperphosphorylated) or U251 (NFI-hypophosphorylated) cells were treated with increasing doses of ACM or calpain inhibitor I (ALLN). After 24 h, the drugs were removed, and cells were allowed to grow for another 12 days. Cells were then fixed and stained with 1% crystal violet in 70% ethanol. Colonies (colony defined as >30 cells) were counted. *B*, cell metabolism, a surrogate for cell viability, was measured using the MTS assay. 3500 U87 (NFI-hyperphosphorylated) or U373 (NFI-hypophosphorylated) cells were seeded in triplicate in 96-well plates. After 24 h, cells were treated with indicated concentrations of ACM. At 36 h post-treatment, cells were incubated with the MTS reagent for an additional 2 h. Fluorescence emission (495 nm) was measured using the FLUOstar Optima plate reader and then normalized to the scrambled siRNA control. Each experiment was repeated three times. (**, p value < 0.01, and ****, p value < 0.0001).

Discussion

Despite extensive research, GBM remains a devastating disease, with low survival time and poor quality of life (44). The lack of improvement in clinical outcome may be attributed to the incomplete understanding of biological processes underlying GBM tumorigenesis and progression, particularly how tumor cells infiltrate normal brain parenchyma. Both calpain and NFI pathways have been shown to play key roles in regulating GBM cell migration. Calpain-mediated proteolysis of downstream effectors is critical for all aspects of cell migration (45, 46). More specific to GBM, calpain 2 is required for tumor cell invasion and infiltration *in vitro* and *in vivo* (47, 48). NFI regulates genes essential for neural cell migration in developing

brain (11, 49). In GBM cells, NFI regulates *FABP7* (12, 13), a gene associated with increased cell migration and worse clinical outcomes in patients (14–17).

In light of (i) the significant intersection of calpain and NFI functions in both normal brain development and GBM and (ii) previous work showing that NFI regulates the gene encoding the endogenous inhibitor of calpain, calpastatin (*CAST*), we hypothesized that cross-signaling occurs between the NFI and calpain pathways. The first empirical evidence supporting NFI–calpain cross-talk was our discovery that NFI transcriptional activity is regulated by calcineurin, which regulates the NFI phosphorylation state (18). Calcineurin is a well-known calpain downstream effector (19, 20, 50, 51). Our subsequent finding that NFI regulates *CAST*, which encodes calpastatin, provided further substantiation for NFI–calpain cross-talk in GBM cells (33).

In this study, we present evidence for a positive feedback loop between NFIB and calpain 1 in GBM cells. Both NFIB and calpain 1 play paradoxical roles in different types of malignancies. For example, whereas NFIB acts as an oncogene in small-cell lung cancer (36), it functions as a tumor suppressor in cutaneous squamous cell carcinoma (52). Similarly, calpain 1 expression has been correlated with both higher and lower survival in different types of breast cancer (53, 54). We found that NFIB can affect calpain 1 activity through two different mechanisms in GBM cells, depending on NFIB phosphorylation state. When NFIB is hyperphosphorylated (Fig. 9A), it down-regulates transcription from an alternative promoter of *CAST*, which contains NFI-binding elements (33). Consequently, *CAST* transcription is primarily initiated at the canonical promoter, resulting in higher levels of full-length calpastatin that has a diffuse cytoplasmic distribution (33). Diffused cytoplasmic calpastatin has been correlated with intracellular activation of calpain (55). Induction of calpain autolysis through suppression of calpastatin expression has previously been demonstrated for the c-Myc transcription factor (56). However, when NFI is hypophosphorylated (Fig. 9B), NFIB promotes transcription from the alternative *CAST* promoter, resulting in higher levels of a truncated form of calpastatin that lacks the XL domain (33). This XL-less calpastatin preferentially localizes to the perinuclear region of the cell (33) and thus is unable to bind and prevent the activation of calpain 1 in other compartments of the cytoplasm. Moreover, the ~55-kDa autolyzed form of calpain 1 detected in our Western blotting experiments has been shown to have lower affinity for calpastatin compared with the full-length form (57). As a result, autolyzed calpain 1 can translocate to the nucleus, further insulating itself from the inhibitory

Figure 7. Effects of calpain 1 depletion on GBM cell migration and viability. U87 (*A*) and U251 (*B*) cells were transfected with scrambled (*CNT*) siRNAs or siRNAs targeting either calpain 1 alone or both calpain 1 and NFIB. *C*, U251 cells were co-transfected with siRNAs (*CNT*, scrambled siRNAs, or *CAPN1-1*, calpain 1-specific siRNA) and DNA constructs (*Empty*, parent pCH vector; *NFIB*, pCH-NFIB expression construct) using the jetPrime reagent. 30,000 U87 (*A*) or U251 (*B* and *C*) cells in fetal calf serum-free DMEM were seeded in the top chambers of Falcon cell culture inserts in a 24-well plate. Directional migration was induced, imaged, and quantified as described in Fig. 4B. Bars, 200 μm. *A* and *B*, *CNT* panels are shared with Fig. 4B as these transfections were carried out at the same time, but are reported separately to focus on the effect of NFIB depletion (Fig. 4B) or calpain 1 depletion (Fig. 7, *A* and *B*) on glioblastoma cell migration. *D*, whole-cell lysates were prepared from U251 cells transiently transfected with scrambled siRNAs or siRNAs targeting calpain 1 (*siCAPN1-1* and *siCAPN1-2*). *E*, whole-cell lysates were prepared from U251 cells transfected with an NFIB expression construct or co-transfected with calpain 1 siRNA and an NFIB expression construct. *D* and *E*, cell lysates were electrophoresed in SDS-polyacrylamide gels and transferred to nitrocellulose membranes. Blots were immunostained with mouse anti-RhoA, rabbit anti-FABP7, and mouse anti-actin antibodies. Numbers represent relative fold changes in densitometric values compared with control transfections ($n = 2$). *F*, U87 and U251 cells were transfected with the indicated siRNAs as outlined in *A* and *B*, respectively. Cell viability was measured using the MTS assay as described in Fig. 4C. Each experiment (except for *D* and *E*) was repeated at least three times. (*n.s.*, p value > 0.05; **, p value < 0.01, and ****, p value < 0.0001).

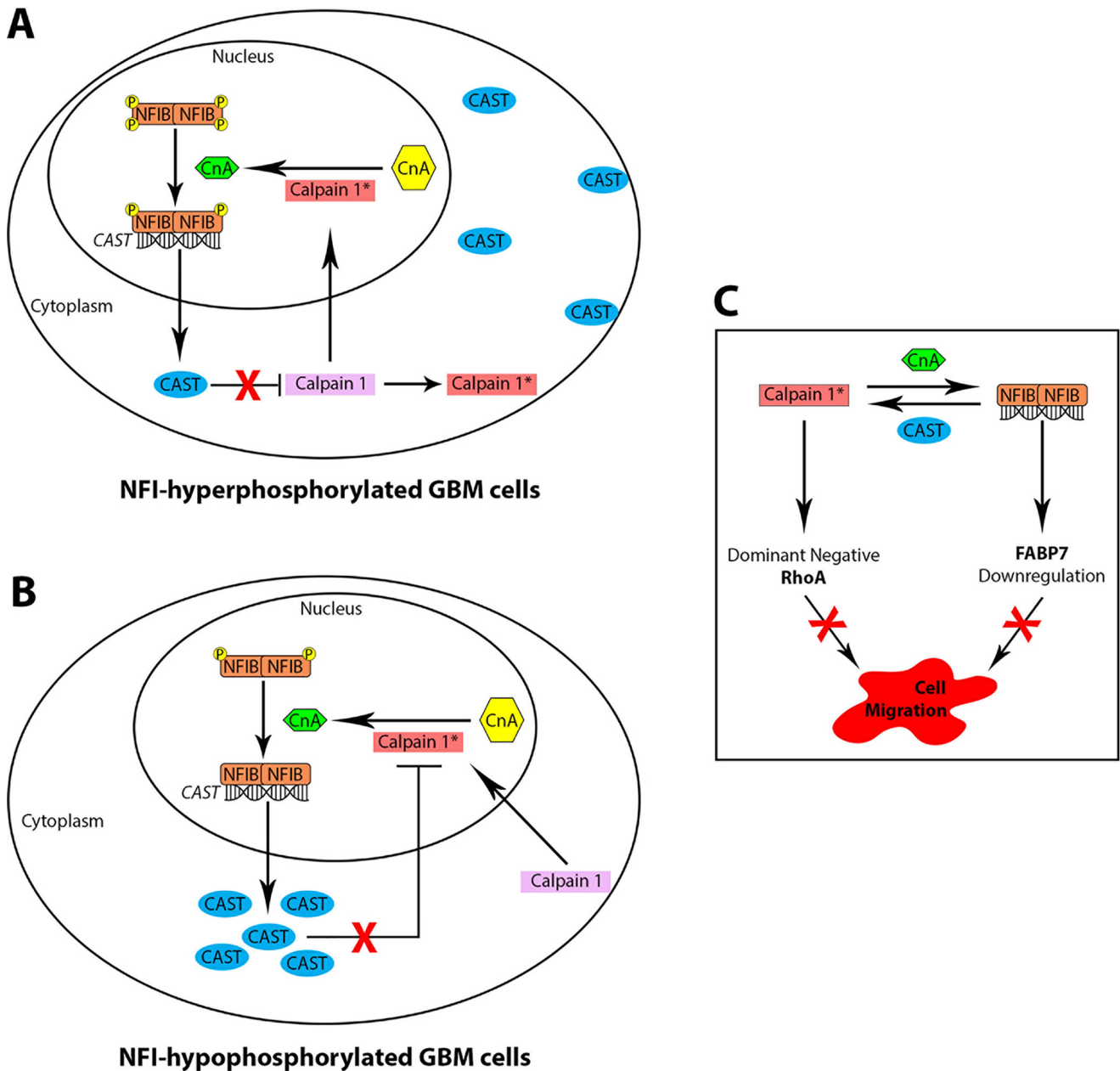


Figure 9. Proposed models for the NFIB–calpain 1-positive feedback loop and how it negatively regulates GBM cell migration. *A*, in NFI-hyperphosphorylated GBM cells, low levels of CnA result in basally-hyperphosphorylated NFIB. CnA, in turn, is cleaved and activated by autolyzed calpain 1 in the nucleus. Hyperphosphorylated NFIB does not up-regulate the alternative promoter containing NFI-binding sites, resulting in higher levels of full-length calpastatin, which has a diffuse distribution in the cytoplasm. Diffused calpastatin is unable to effectively prevent the autolysis and activation of full-length calpain 1, resulting in a small amount of autolyzed calpain 1. This autolyzed calpain 1, with low affinity for calpastatin, translocates into the nucleus resulting in low levels of CnA activation, repeating the signaling cycle. *B*, in NFI-hypophosphorylated GBM cells, NFIB is dephosphorylated by high levels of CnA in the nucleus. Hypophosphorylated NFIB up-regulates the alternative *CAST* promoter, resulting in increased levels of a truncated form of calpastatin that lacks the XL domain. This XL-less calpastatin preferentially localizes to the perinuclear region of the cell. As a result, calpastatin is unable to bind calpain 1 in other compartments of the cytoplasm. The majority of free cytoplasmic calpain 1 undergoes autolysis, producing high levels of autolyzed calpain 1. The latter accumulates in the nucleus, resulting in increased levels of cleaved and activated CnA, which in turn further dephosphorylates NFIB, perpetuating the positive feedback loop. *C*, calpain 1–NFIB-positive feedback loop negatively regulates GBM cell migration through calpain 1-mediated proteolysis of RhoA (generating a dominant-negative fragment) and NFIB-mediated down-regulation of *FABP7* expression.

activity of calpastatin. Thus, our combined data suggest that although mechanistically different, both hyper- and hypophosphorylated NFIB can enhance calpain 1 activity. In support of an NFIB–calpain 1-positive feedback loop in GBM, we also found that calpain 1 can affect NFIB phosphorylation. We have previously shown that NFIB phosphorylation affects its transcriptional activity (12, 13). Thus, calpain 1 cleaves and activates calcineurin, which in turn dephosphorylates NFIB and

perpetuates the signaling cycle. Whether calpain 1-induced and calcineurin-mediated dephosphorylation can be extended to members of the NFI family other than NFIB remains to be examined.

Evidence from the literature suggests various roles for NFIB in cancer cell migration. For example, NFIB enhances migration of tumor cells by changing chromatin state and accessibility (58, 59). However, NFIB expression can also be inversely

NFIB–calpain 1-positive feedback loop in GBM cells

correlated with cell migration and invasion, as demonstrated in osteosarcoma (60). In line with the latter observation, we show that NFIB negatively regulates GBM cell migration by down-regulating the expression of GBM pro-migratory protein FABP7. Intriguingly, hypophosphorylated NFIs have previously been shown to up-regulate, not down-regulate, *FABP7* expression in GBM cells (12). However, closer examination of the data in this paper shows similar results to those reported here, *i.e.* up-regulation of *FABP7* upon NFIB depletion. Brun *et al.* (12) attributed the effect of NFIB on *FABP7* to possible interplay between the various members of the NFI family. However, in light of our new data, a more likely explanation is that different members of the NFI family play different roles in GBM cells. Thus, NFIB, as a negative regulator of *FABP7*, may counteract the oncogenic effect of other NFI members. Also, in agreement with our results, there is a correlation between higher levels of NFIB and increased survival in patients with classical and mesenchymal GBM tumors (35). Because both U87 and U251 are of the mesenchymal GBM subtype (61, 62), the association between NFIB expression and better clinical outcomes may be explained in part by NFIB-mediated down-regulation of *FABP7* expression, resulting in reduced GBM cell migration.

Similar to NFIB, the role of calpain 1 in regulating cell migration varies depending on the system being analyzed, perhaps due to functional compensation provided by other calpain members. Whereas a number of studies have established calpain 2 as an essential promoter of GBM cell migration, this work may be the first to implicate calpain 1 as a negative regulator of cell migration in GBM. A few reports in other systems support an anti-migratory role for calpain 1. For example, in bovine aortic endothelial cells, calpain 1 can cleave and generate a dominant-negative fragment of RhoA that inhibits cell spreading (25). Although we were not able to detect the cleaved form of RhoA in GBM cells, possibly due to the instability of calpain 1–proteolyzed RhoA, we did observe increased levels of full-length RhoA upon calpain 1 depletion in GBM cells. Calpain 1 depletion in GBM cells also led to an increase in the expression of pro-migratory *FABP7*. These combined observations support a link between NFIB, calpain 1, and RhoA/*FABP7*-mediated cell migration.

Over the last few decades, there has been increasing interest in using calpain activators and inhibitors for clinical purposes (22, 29, 63), with attention focusing on using calpain inhibitors for the treatment of many pathological conditions, including neurodegenerative diseases and cancer. Our colony formation assay indicates that calpain inhibitors ACM and ALLN can be used to significantly reduce GBM cell survival. NFIs, like many other transcription factors, remain largely undruggable. Consequently, the existence of cross-talk between NFI and calpain may allow targeting of these key pathways with calpain inhibitors. However, our Transwell and colony formation data suggest that inhibiting both calpains 1 and 2 may also cause increased tumor cell migration, a hallmark of tumor infiltration. As the NFIB–calpain 1-positive feedback loop in GBM cells appears to suppress tumor cell migration, we suggest that a calpain 1-specific agonist holds the most promise for targeting infiltrative GBM cells. Opposite effects for calpain 1 and calpain 2 have been observed in both neurodegeneration and

synaptic plasticity: calpain 1 is neuroprotective and induces long-term potentiation (LTP), in contrast to calpain 2, which promotes neurodegeneration and restricts LTP (64). In the context of brain development, calpain 1 acts to maintain the self-renewing capacity of neural stem cells, whereas calpain 2 promotes the differentiation of these cells (65).

In summary, we report a positive NFIB–calpain 1 feedback loop in GBM cell lines. Our results shed light on the molecular basis of the signaling pathways of this cross-talk, with calpain 1 inducing NFIB dephosphorylation through cleavage and activation of calcineurin and NFIB increasing calpain 1 activity through *CAST*-mediated regulation of calpastatin levels and subcellular localization. We also provide evidence that NFIB, through NFIB-mediated down-regulation of *FABP7*, and calpain 1, likely through calpain 1-mediated proteolysis of RhoA into its dominant-negative form (Fig. 9C), act in concert to suppress GBM cell migration. Finally, our data suggest that inhibitors targeting both calpains 1 and 2, although useful for reducing tumor mass, may not be of benefit in controlling GBM cell migration and infiltration.

Experimental procedures

Cell lines, constructs, transfections, and treatments

T98, U87, U251, and U373 GBM cell lines have been described elsewhere (12, 66). Cells were cultured in Dulbecco's modified Eagle's minimum essential medium supplemented with 8% fetal bovine serum (FBS), streptomycin (50 μ g/ml), and penicillin (50 units/ml). pCH-NFI expression constructs were a generous gift from Dr. R. Gronostajski (Case Western Reserve University). GBM cells were transfected with pCH empty vector or NFI-expression constructs using polyethyleneimine (PEI) (Polysciences) with a ratio of 5:1 (μ g of PEI/ μ g of DNA). Co-transfection of calpain 1 siRNA and NFIB expression construct (pCH-NFIB) was carried out using the jetPrime reagent (VWR International). Cells were harvested 60 h post-transfection.

Knockdown of endogenous NFIs and CAPN1

GBM cells were transfected with the following siRNAs (Life Technologies, Inc.): scrambled (control) siRNAs (catalog nos. 12935-200 and 12935-300); NFIA, NM_005595_stealth_919 (5'-GAAAGUUCUUCUACUACAGCAUGA-3'); NFIB-1, NM_005596_stealth_1020 (5'-AAGCCACAAUGAUCCUGCCAAGAAU-3'); NFIB-2, NIFBHSS107131 (5'-GCUGGAGUCGAACAUGGCACGAAA-3'); NFIC, NM_005597_stealth_1045 (5'-CAGAGAUGGACAAGUCACCAUUCAA-3'); NFIX, NM_002501_stealth_752 (5'-GAGAGUAUCACAGACUCCUGUUGCA-3'); CAPN1-1, CAPN1HSS188701 (5'-CAGAGUGGAACAACGUGGACCCAUA-3'); and CAPN1-2, CAPN1HSS101345 (5'-CCGUACCACUUGAAGCGUGACUUCUU-3'). Ten nM of each siRNA was introduced into GBM cells using the RNAiMAX Lipofectamine reagent (Invitrogen) according to the manufacturer's instruction. Cells were trypsinized and replated 48 h post-transfection (1:6) for the second round of siRNA. Cells were harvested 60 h after the second transfection.

Table 1
Primer sequences

Locus	Forward primer (5' to 3')	Reverse primer (5' to 3')
<i>GAPDH</i>	ACCAGGGAGGGCTGCAGT	CAGTTCGGAGCCACACCG
<i>CAPN1</i>	CACCACACTCTACGAAGGCA	ACGCTCAAGTGTACGGCC
<i>CAPN2</i>	TAACGGGAAGCCTACAGAAACT	TTTTTGCTGAGGTGGATGTTG
<i>CAPNS1</i>	CCAACGAGAGTGAGGAGGT	TGACCAAGCAGCTGATGAAG
<i>ACTB</i>	CTGGCACACACCTTCTAC	CATACTCCTGCTTGCTGATC

Reverse transcription (RT) and qPCR

The TRIzol[®] reagent (Thermo Fisher Scientific) was used to isolate total RNA from GBM cells. First-strand cDNA synthesis was carried out with Superscript II[®] reverse transcriptase (Invitrogen). For RT-PCR, primers specific to *CAPN1*, *CAPN2*, *CAPNS1*, and *ACTB* were used to amplify cDNA (Table 1). For RT-qPCR, cDNAs were amplified using primers flanking a unique region of *CAPN1* with the BrightGreen[®] qPCR master mix (ABM Scientific). Raw signals were first normalized to *GAPDH* and then to the respective scrambled siRNA control to generate relative fold change data.

Western blot analysis

Whole-cell lysates were prepared by lysing cells in modified RIPA buffer (50 mM Tris-HCl, pH 7.5, 1% sodium deoxycholate, 1% Triton X-100, 150 mM NaCl, 50 mM sodium fluoride, 1 mM sodium orthovanadate, 10 mM EDTA, 0.1% SDS, 0.5 mM phenylmethylsulfonyl fluoride, 1× cOmplete protease inhibitor (Roche Applied Science), and 1× PhosSTOP phosphatase inhibitor (Roche Applied Science)). For λ-phosphatase (New England Biolabs) treatment, 10 μg of nuclear lysates were incubated with either water (negative control) or 400 units of λ-phosphatase for 1 h at 30 °C in the supplied reaction buffer, supplemented with 1 mM MnCl₂. Whole-cell and nuclear lysates were resolved in SDS-polyacrylamide gels and transferred to nitrocellulose membranes. Blots were then immunostained with the following: rabbit anti-calpastatin antibody (1:5000, Abcam, catalog no. ab5582); mouse anti-calpain 1 antibody (1:500, Santa Cruz Biotechnology, catalog no. sc-271313); rabbit anti-calpain 2 antibody (1:1000, Santa Cruz Biotechnology, catalog no. sc-30064); mouse anti-calcineurin antibody (1:1000, Pharmingen, clone G182-1847); rabbit anti-NFIB antibody (1:2500, Invitrogen, catalog no. PA5-52032); mouse anti-RhoA antibody (1:500, Santa Cruz Biotechnology, catalog no. sc-418); mouse anti-lamin A/C antibody (1:1000, Thermo Fisher Scientific, catalog no. MA3-1000); mouse anti-α-tubulin (1:100,000, Hybridoma Bank, clone 12G10); or mouse anti-β-actin antibody (1:100,000, Sigma, clone AC-15). Proteins of interest were visualized using horseradish peroxidase-conjugated secondary antibody (Jackson ImmunoResearch Biotech) with the Immobilon (EMD Millipore) or ECL (GE Healthcare) chemiluminescent HRP substrate.

Cytoplasmic and nuclear fractionation

Nuclear and cytoplasmic fractionation was carried out using the NE-PER kit (Thermo Fisher Scientific) with modification for nuclear fractionation. Briefly, cytoplasmic lysates were prepared using the supplied reagents supplemented with 1× cOmplete protease inhibitors and 1× PhosSTOP. Nuclei were

obtained by centrifugation of cytoplasmic lysates. Purified nuclei were lysed in modified RIPA buffer as described above. For λ-phosphatase treatment, cytoplasmic and nuclear fractionation was carried out in the absence of EDTA and phosphatase inhibitors (sodium fluoride, sodium orthovanadate, and PhosSTOP). To shear chromatin, nuclear lysates were subjected to 20 cycles of sonication at 4 °C (high output, 30 s power on and 30 s power off) using a Bioruptor 300[®] sonicator (Diagenode). Nuclear debris was pelleted by centrifugation. The supernatant was then removed and used as nuclear lysates.

Calpain activity assay

Calpain proteolytic activity was measured using the fluorogenic calpain activity assay kit (Calbiochem). Briefly, whole-cell lysates were prepared from U87 and U251 GBM cells using the supplied lysis buffer. Changes in fluorescence intensity upon substrate cleavage was measured in buffers that promote (Activation buffer) or suppress (Inhibition buffer) calpain activity using the FLUOstar Optima microplate reader (355 nm excitation and 480 nm emission, BMG Labtech). Raw data obtained with the Activation buffer were normalized against those obtained with the Inhibition buffer. Relative fold change in fluorescence intensity was generated by normalizing each data point to the respective scrambled siRNA control.

Transwell migration assay

U251 and U87 GBM cells were transfected with the indicated siRNAs and plasmid-based expression constructs. Thirty thousand cells in FBS-free DMEM were seeded in the top chamber of Falcon cell culture inserts (Thermo Fisher Scientific). Cells were allowed to migrate through an 8-μm polyethylene terephthalate membrane toward a chemoattractant (DMEM + 10% fetal calf serum) in the bottom chamber for 20 h. Cells were then fixed with 100% cold methanol for 20 min and stained with 1% crystal violet in 20% methanol for 30 min. Migrated cells were imaged using a Zeiss Axioskop2 plus microscope using multiple fields covering the whole surface of the inserts. Cell counting was carried out using MetaMorph software (Molecular Devices).

MTS assay

U87, T98, U251, and U373 GBM cells were transfected with the indicated siRNAs as described previously or treated with the indicated concentrations of ACM. Cell metabolism, a surrogate of cell viability, was measured using the CellTiter 96[®] nonradioactive cell proliferation MTS assay (Promega). Briefly, ~3500 siRNA-transfected cells were seeded in 96-well plates in triplicate and allowed to grow for 48 h. For ACM treatment, ~3500 cells were seeded and allowed to recover for 24 h and then incubated with the drug for an additional 36 h. Next, 20 μl of MTS reagent was added to each well and then incubated for an additional 2 h. Absorbance was measured using the FLUOstar OPTIMA microplate reader with the absorbance wavelength of 495 nm. Relative fold change was generated by normalizing absorbance values to their respective scrambled siRNA or DMSO controls.

NFIB–calpain 1-positive feedback loop in GBM cells

Colony formation assay

The colony formation assay was carried out as previously described (67). Briefly, ~500 T98 or U251 GMB cells were plated in triplicate and treated with the indicated doses of ACM or ALLN. After 24 h, the medium was changed followed by washing with PBS to remove traces of drug. Cells were allowed to grow for an additional 12 days and then fixed and stained with 1% crystal violet in 70% ethanol. Colonies (>30 cells) were counted.

Immunofluorescence analysis

For immunofluorescence analysis, siRNA-transfected GBM cells were plated onto glass coverslips. Cells were allowed to recover for 24 h and then fixed with 4% paraformaldehyde for 10 min at room temperature. Cells were then permeabilized with 0.25% Triton X-100 for 4 min. To reduce background staining, cells were blocked with 3% BSA for 45 min at room temperature. Cells were then immunostained with rabbit anti-calpastatin (1:100, Santa Cruz Biotechnology, catalog no. sc-20779), mouse anti-calpain 1 antibody (1:10, Santa Cruz Biotechnology, catalog no. sc-271313), mouse anti-calceinurin antibody (1:50, Pharmingen, clone G182-1847), and rabbit anti-NFIB antibody (1:400, Life Technologies, Inc., catalog no. PA5-52032). Signals were visualized using Alexa 488–conjugated donkey anti-rabbit or Alexa 555–conjugated donkey anti-mouse secondary antibodies (both at 1:400, Life Technologies, Inc.). Nuclei were stained with 4',6-diamidino-2-phenylindole (DAPI, Calbiochem). Images were acquired with a ×40/1.3 oil immersion objective lens on a Zeiss LSM 710 confocal microscope using Zeiss ZEN imaging software. For quantification of calpain 1 and calcineurin subcellular localization, fluorescence signal intensity values were calculated for at least 300 cells (100 cells for each biological replicate) using the MetaXpress software (Molecular Devices), with DAPI being used as the marker for the nuclear region. Data are presented as relative percentage of nuclear over cytoplasmic fluorescence intensity. For quantification of NFIB nucleolus localization, at least 300 random cells (100 cells for each biological replicate) were assessed for the absence of NFIB immunostaining in the nucleolus region. Data are presented as percentage of cells negative for nucleolar NFIB related to total number of cells counted.

Author contributions—T. M. V., R. B., and R. G. conceptualization; T. M. V., S. J., and E. A. M. data curation; T. M. V. and S. J. formal analysis; T. M. V. validation; T. M. V. investigation; T. M. V. visualization; T. M. V., S. J., R. B., and E. A. M. methodology; T. M. V. and R. G. writing-original draft; T. M. V., S. J., R. B., E. A. M., and R. G. writing-review and editing; R. G. resources; R. G. supervision; R. G. funding acquisition; R. G. project administration.

Acknowledgments—We thank Dr. R. Gronostajski (Case Western Reserve University) for the NFIB expression constructs. We are grateful to Dr. Xuejun Sun, Gerry Barron, and the Cross Cancer Institute Cell Imaging Facility for their support with imaging GBM cells.

References

1. Omuro, A., and DeAngelis, L. M. (2013) Glioblastoma and other malignant gliomas: a clinical review. *JAMA* **310**, 1842–1850 [CrossRef Medline](#)

- Ostrom, Q. T., Gittleman, H., Fulop, J., Liu, M., Blanda, R., Kromer, C., Wolinsky, Y., Kruchko, C., and Barnholtz-Sloan, J. S. (2015) CBTRUS statistical report: primary brain and central nervous system tumors diagnosed in the United States in 2008–2012. *Neuro Oncol.* **17**, Suppl. 4, iv1–iv62 [CrossRef Medline](#)
- Mason, W. P., Maestro, R. D., Eisenstat, D., Forsyth, P., Fulton, D., Laperrière, N., Macdonald, D., Perry, J., Thiessen, B., and Canadian GBM Recommendations Committee. (2007) Canadian recommendations for the treatment of glioblastoma multiforme. *Curr. Oncol.* **14**, 110–117 [CrossRef Medline](#)
- Claes, A., Idema, A. J., and Wesseling, P. (2007) Diffuse glioma growth: a guerilla war. *Acta Neuropathol.* **114**, 443–458 [CrossRef Medline](#)
- de Groot, J. F., Fuller, G., Kumar, A. J., Piao, Y., Eterovic, K., Ji, Y., and Conrad, C. A. (2010) Tumor invasion after treatment of glioblastoma with bevacizumab: radiographic and pathologic correlation in humans and mice. *Neuro Oncol.* **12**, 233–242 [CrossRef Medline](#)
- Kallenberg, K., Goldmann, T., Menke, J., Strik, H., Bock, H. C., Stockhammer, F., Buhk, J. H., Frahm, J., Dechent, P., and Knauth, M. (2013) Glioma infiltration of the corpus callosum: early signs detected by DTI. *J. Neurooncol.* **112**, 217–222 [CrossRef Medline](#)
- Norden, A. D., Young, G. S., Setayesh, K., Muzikansky, A., Klufas, R., Ross, G. L., Ciampa, A. S., Ebbeling, L. G., Levy, B., Drappatz, J., Kesari, S., and Wen, P. Y. (2008) Bevacizumab for recurrent malignant gliomas: efficacy, toxicity, and patterns of recurrence. *Neurology* **70**, 779–787 [CrossRef Medline](#)
- Ogura, K., Mizowaki, T., Arakawa, Y., Ogura, M., Sakanaka, K., Miyamoto, S., and Hiraoka, M. (2013) Initial and cumulative recurrence patterns of glioblastoma after temozolomide-based chemoradiotherapy and salvage treatment: a retrospective cohort study in a single institution. *Radiat. Oncol.* **8**, 97 [CrossRef Medline](#)
- Shankar, A., Kumar, S., Iskander, A. S., Varma, N. R., Janic, B., deCarvalho, A., Mikkelsen, T., Frank, J. A., Ali, M. M., Knight, R. A., Brown, S., and Arbab, A. S. (2014) Subcurative radiation significantly increases cell proliferation, invasion, and migration of primary glioblastoma multiforme *in vivo*. *Chin. J. Cancer* **33**, 148–158 [CrossRef Medline](#)
- Gronostajski, R. M. (2000) Roles of the NFIB/CTF gene family in transcription and development. *Gene* **249**, 31–45 [CrossRef Medline](#)
- Mason, S., Piper, M., Gronostajski, R. M., and Richards, L. J. (2009) Nuclear factor one transcription factors in CNS development. *Mol. Neurobiol.* **39**, 10–23 [CrossRef Medline](#)
- Brun, M., Coles, J. E., Monckton, E. A., Glubrecht, D. D., Bisgrove, D., and Godbout, R. (2009) Nuclear factor I regulates brain fatty acid-binding protein and glial fibrillary acidic protein gene expression in malignant glioma cell lines. *J. Mol. Biol.* **391**, 282–300 [CrossRef Medline](#)
- Bisgrove, D. A., Monckton, E. A., Packer, M., and Godbout, R. (2000) Regulation of brain fatty acid-binding protein expression by differential phosphorylation of nuclear factor I in malignant glioma cell lines. *J. Biol. Chem.* **275**, 30668–30676 [CrossRef Medline](#)
- Liang, Y., Bollen, A. W., Aldape, K. D., and Gupta, N. (2006) Nuclear FABP7 immunoreactivity is preferentially expressed in infiltrative glioma and is associated with poor prognosis in EGFR-overexpressing glioblastoma. *BMC Cancer* **6**, 97 [CrossRef Medline](#)
- De Rosa, A., Pellegatta, S., Rossi, M., Tunici, P., Magnoni, L., Speranza, M. C., Malusa, F., Miragliotta, V., Mori, E., Finocchiaro, G., and Bakker, A. (2012) A radial glia gene marker, fatty acid binding protein 7 (FABP7), is involved in proliferation and invasion of glioblastoma cells. *PLoS ONE* **7**, e52113 [CrossRef Medline](#)
- Kaloshi, G., Mokhtari, K., Carpentier, C., Taillibert, S., Lejeune, J., Marie, Y., Delattre, J. Y., Godbout, R., and Sanson, M. (2007) FABP7 expression in glioblastomas: relation to prognosis, invasion and EGFR status. *J. Neurooncol.* **84**, 245–248 [CrossRef Medline](#)
- Mita, R., Beaulieu, M. J., Field, C., and Godbout, R. (2010) Brain fatty acid-binding protein and omega-3/omega-6 fatty acids: mechanistic insight into malignant glioma cell migration. *J. Biol. Chem.* **285**, 37005–37015 [CrossRef Medline](#)
- Brun, M., Glubrecht, D. D., Baksh, S., and Godbout, R. (2013) Calcineurin regulates nuclear factor I dephosphorylation and activity in malignant glioma cell lines. *J. Biol. Chem.* **288**, 24104–24115 [CrossRef Medline](#)

19. Wu, H. Y., Tomizawa, K., Oda, Y., Wei, F. Y., Lu, Y. F., Matsushita, M., Li, S. T., Moriwaki, A., and Matsui, H. (2004) Critical role of calpain-mediated cleavage of calcineurin in excitotoxic neurodegeneration. *J. Biol. Chem.* **279**, 4929–4940 [CrossRef Medline](#)
20. Kim, M. J., Jo, D. G., Hong, G. S., Kim, B. J., Lai, M., Cho, D. H., Kim, K. W., Bandyopadhyay, A., Hong, Y. M., Kim, D. H., Cho, C., Liu, J. O., Snyder, S. H., and Jung, Y. K. (2002) Calpain-dependent cleavage of cain/cabin1 activates calcineurin to mediate calcium-triggered cell death. *Proc. Natl. Acad. Sci. U.S.A.* **99**, 9870–9875 [CrossRef Medline](#)
21. Goll, D. E., Thompson, V. F., Li, H., Wei, W., and Cong, J. (2003) The calpain system. *Physiol. Rev.* **83**, 731–801 [CrossRef Medline](#)
22. Storr, S. J., Carragher, N. O., Frame, M. C., Parr, T., and Martin, S. G. (2011) The calpain system and cancer. *Nat. Rev. Cancer* **11**, 364–374 [CrossRef Medline](#)
23. Croce, K., Flaumenhaft, R., Rivers, M., Furie, B., Furie, B. C., Herman, I. M., and Potter, D. A. (1999) Inhibition of calpain blocks platelet secretion, aggregation, and spreading. *J. Biol. Chem.* **274**, 36321–36327 [CrossRef Medline](#)
24. Lokuta, M. A., Nuzzi, P. A., and Huttenlocher, A. (2003) Calpain regulates neutrophil chemotaxis. *Proc. Natl. Acad. Sci. U.S.A.* **100**, 4006–4011 [CrossRef Medline](#)
25. Kulkarni, S., Goll, D. E., and Fox, J. E. (2002) Calpain cleaves RhoA generating a dominant-negative form that inhibits integrin-induced actin filament assembly and cell spreading. *J. Biol. Chem.* **277**, 24435–24441 [CrossRef Medline](#)
26. Li, H., Thompson, V. F., and Goll, D. E. (2004) Effects of autolysis on properties of μ - and m-calpain. *Biochim. Biophys. Acta* **1691**, 91–103 [CrossRef Medline](#)
27. Wendt, A., Thompson, V. F., and Goll, D. E. (2004) Interaction of calpastatin with calpain: a review. *Biol. Chem.* **385**, 465–472 [CrossRef Medline](#)
28. Melloni, E., Michetti, M., Salamino, F., Minafra, R., and Pontremoli, S. (1996) Modulation of the calpain autoproteolysis by calpastatin and phospholipids. *Biochem. Biophys. Res. Commun.* **229**, 193–197 [CrossRef Medline](#)
29. Donkor, I. O. (2011) Calpain inhibitors: a survey of compounds reported in the patent and scientific literature. *Expert Opin. Ther. Pat.* **21**, 601–636 [CrossRef Medline](#)
30. Figueiredo-Pereira, M. E., Chen, W. E., Li, J., and Johdo, O. (1996) The antitumor drug acalincinomyacin A, which inhibits the degradation of ubiquitinated proteins, shows selectivity for the chymotrypsin-like activity of the bovine pituitary 20 S proteasome. *J. Biol. Chem.* **271**, 16455–16459 [CrossRef Medline](#)
31. Staib, P., Lathan, B., Knöppel-Schwark, S., Tesch, H., Voliotis, D., Steinmetz, H. T., Schwonzen, M., Wickramanayake, P. D., and Diehl, V. (1998) Cytosine arabinoside, etoposide and aclarubicin (AVA) for the treatment of acute myeloid leukemia (AML) in elderly patients. *Ann. Oncol.* **9**, 221–223 [CrossRef Medline](#)
32. Röthig, H. J., Kraemer, H. P., and Sedlacek, H. H. (1985) Aclarubicin: experimental and clinical experience. *Drugs Exp. Clin. Res.* **11**, 123–125 [Medline](#)
33. Vo, T. M., Burchett, R., Brun, M., Monckton, E. A., Poon, H. Y., and Godbout, R. (2019) Effects of nuclear factor I phosphorylation on calpastatin (CAST) gene variant expression and subcellular distribution in malignant glioma cells. *J. Biol. Chem.* **294**, 1173–1188 [CrossRef Medline](#)
34. Brun, M., Jain, S., Monckton, E. A., and Godbout, R. (2018) Nuclear factor I represses the Notch effector HEY1 in glioblastoma. *Neoplasia* **20**, 1023–1037 [CrossRef Medline](#)
35. Stringer, B. W., Bunt, J., Day, B. W., Barry, G., Jamieson, P. R., Ensby, K. S., Bruce, Z. C., Goasdoué, K., Vidal, H., Charmsaz, S., Smith, F. M., Cooper, L. T., Piper, M., Boyd, A. W., and Richards, L. J. (2016) Nuclear factor one B (NFIB) encodes a subtype-specific tumour suppressor in glioblastoma. *Oncotarget* **7**, 29306–29320 [CrossRef Medline](#)
36. Dooley, A. L., Winslow, M. M., Chiang, D. Y., Banerji, S., Stransky, N., Dayton, T. L., Snyder, E. L., Senna, S., Whittaker, C. A., Bronson, R. T., Crowley, D., Barretina, J., Garraway, L., Meyerson, M., and Jacks, T. (2011) Nuclear factor I/B is an oncogene in small cell lung cancer. *Genes Dev.* **25**, 1470–1475 [CrossRef Medline](#)
37. Liu, R. Z., Vo, T. M., Jain, S., Choi, W. S., Garcia, E., Monckton, E. A., Mackey, J. R., and Godbout, R. (2019) NFIB promotes cell survival by directly suppressing p21 transcription in TP53-mutated triple-negative breast cancer. *J. Pathol.* **247**, 186–198 [CrossRef Medline](#)
38. Averna, M., De Tullio, R., Capini, P., Salamino, F., Pontremoli, S., and Melloni, E. (2003) Changes in calpastatin localization and expression during calpain activation: a new mechanism for the regulation of intracellular Ca²⁺-dependent proteolysis. *Cell. Mol. Life Sci.* **60**, 2669–2678 [CrossRef Medline](#)
39. Averna, M., de Tullio, R., Passalacqua, M., Salamino, F., Pontremoli, S., and Melloni, E. (2001) Changes in intracellular calpastatin localization are mediated by reversible phosphorylation. *Biochem. J.* **354**, 25–30 [CrossRef Medline](#)
40. Riss, T. L., Moravec, R. A., Niles, A. L., Duellman, S., Benink, H. A., Worzella, T. J., and Minor, L. (2004) in *Assay Guidance Manual* (Sittampalam, G. S., Coussens, N. P., Brimacombe, K., Grossman, A., Arkin, M., eds, *et al.*) pp. 289–314
41. Talamillo, A., Grande, L., Ruiz-Ontañón, P., Velasquez, C., Mollinedo, P., Torices, S., Sanchez-Gomez, P., Aznar, A., Esparis-Ogando, A., Lopez-Lopez, C., Lafita, C., Berciano, M. T., Montero, J. A., Vazquez-Barquero, A., Segura, V., Villagra, N. T., *et al.* (2017) ODZ1 allows glioblastoma to sustain invasiveness through a Myc-dependent transcriptional upregulation of RhoA. *Oncogene* **36**, 1733–1744 [CrossRef Medline](#)
42. Yoshioka, K., Nakamori, S., and Itoh, K. (1999) Overexpression of small GTP-binding protein RhoA promotes invasion of tumor cells. *Cancer Res.* **59**, 2004–2010 [Medline](#)
43. Mita, R., Coles, J. E., Glubrecht, D. D., Sung, R., Sun, X., and Godbout, R. (2007) B-FABP-expressing radial glial cells: the malignant glioma cell of origin? *Neoplasia* **9**, 734–744 [CrossRef Medline](#)
44. Liu, R., Page, M., Solheim, K., Fox, S., and Chang, S. M. (2009) Quality of life in adults with brain tumors: current knowledge and future directions. *Neuro Oncol.* **11**, 330–339 [CrossRef Medline](#)
45. Sheetz, M. P., Felsenfeld, D., Galbraith, C. G., and Choquet, D. (1999) Cell migration as a five-step cycle. *Biochem. Soc. Symp.* **65**, 233–243 [Medline](#)
46. Franco, S. J., and Huttenlocher, A. (2005) Regulating cell migration: calpains make the cut. *J. Cell Sci.* **118**, 3829–3838 [CrossRef Medline](#)
47. Franco, S., Perrin, B., and Huttenlocher, A. (2004) Isoform specific function of calpain 2 in regulating membrane protrusion. *Exp. Cell Res.* **299**, 179–187 [CrossRef Medline](#)
48. Lal, S., La Du, J., Tanguay, R. L., and Greenwood, J. A. (2012) Calpain 2 is required for the invasion of glioblastoma cells in the zebrafish brain microenvironment. *J. Neurosci. Res.* **90**, 769–781 [CrossRef Medline](#)
49. Heng, Y. H., Barry, G., Richards, L. J., and Piper, M. (2012) Nuclear factor I genes regulate neuronal migration. *Neurosignals* **20**, 159–167 [CrossRef Medline](#)
50. Ding, F., Li, X., Li, B., Guo, J., Zhang, Y., and Ding, J. (2016) Calpain-mediated cleavage of calcineurin in puromycin aminonucleoside-induced podocyte injury. *PLoS ONE* **11**, e0155504 [CrossRef Medline](#)
51. Wu, H. Y., Tomizawa, K., and Matsui, H. (2007) Calpain-calcineurin signaling in the pathogenesis of calcium-dependent disorder. *Acta Med. Okayama* **61**, 123–137 [CrossRef Medline](#)
52. Zhou, M., Zhou, L., Zheng, L., Guo, L., Wang, Y., Liu, H., Ou, C., and Ding, Z. (2014) miR-365 promotes cutaneous squamous cell carcinoma (CSCC) through targeting nuclear factor I/B (NFIB). *PLoS ONE* **9**, e100620 [CrossRef Medline](#)
53. Storr, S. J., Zhang, S., Perren, T., Lansdown, M., Fatayer, H., Sharma, N., Gahlaut, R., Shaaban, A., and Martin, S. G. (2016) The calpain system is associated with survival of breast cancer patients with large but operable inflammatory and non-inflammatory tumours treated with neoadjuvant chemotherapy. *Oncotarget* **7**, 47927–47937 [CrossRef Medline](#)
54. Pu, X., Storr, S. J., Ahmad, N. S., Chan, S. Y., Moseley, P. M., Televantou, D., Cresti, N., Boddy, A., Ellis, I. O., and Martin, S. G. (2016) Calpain-1 is associated with adverse relapse free survival in breast cancer: a confirmatory study. *Histopathology* **68**, 1021–1029 [CrossRef Medline](#)
55. Stifanese, R., Averna, M., De Tullio, R., Pedrazzi, M., Beccaria, F., Salamino, F., Milanese, M., Bonanno, G., Pontremoli, S., and Melloni, E. (2010) Adaptive modifications in the calpain/calpastatin system in brain cells

NFIB–calpain 1-positive feedback loop in GBM cells

- after persistent alteration in Ca^{2+} homeostasis. *J. Biol. Chem.* **285**, 631–643 [CrossRef Medline](#)
56. Yang, B. S., Gilbert, J. D., and Freytag, S. O. (1993) Overexpression of Myc suppresses CCAAT transcription factor/nuclear factor 1-dependent promoters *in vivo*. *Mol. Cell. Biol.* **13**, 3093–3102 [CrossRef Medline](#)
57. Nishimura, T., and Goll, D. E. (1991) Binding of calpain fragments to calpastatin. *J. Biol. Chem.* **266**, 11842–11850 [Medline](#)
58. Denny, S. K., Yang, D., Chuang, C. H., Brady, J. J., Lim, J. S., Grüner, B. M., Chiou, S. H., Schep, A. N., Baral, J., Hamard, C., Antoine, M., Wislez, M., Kong, C. S., Connolly, A. J., Park, K. S., Sage, J., *et al.* (2016) Nfib promotes metastasis through a widespread increase in chromatin accessibility. *Cell* **166**, 328–342 [CrossRef Medline](#)
59. Fane, M. E., Chhabra, Y., Hollingsworth, D. E. J., Simmons, J. L., Spoerri, L., Oh, T. G., Chauhan, J., Chin, T., Harris, L., Harvey, T. J., Muscat, G. E. O., Goding, C. R., Sturm, R. A., Haass, N. K., Boyle, G. M., *et al.* (2017) NFIB mediates BRN2 driven melanoma cell migration and invasion through regulation of EZH2 and MITF. *EBioMedicine* **16**, 63–75 [CrossRef Medline](#)
60. Mirabello, L., Koster, R., Moriarity, B. S., Spector, L. G., Meltzer, P. S., Gary, J., Machiela, M. J., Pankratz, N., Panagiotou, O. A., Largaespada, D., Wang, Z., Gastier-Foster, J. M., Gorlick, R., Khanna, C., de Toledo, S. R., *et al.* (2015) A genome-wide scan identifies variants in NFIB associated with metastasis in patients with osteosarcoma. *Cancer Discov.* **5**, 920–931 [CrossRef Medline](#)
61. Ge, L., Cornforth, A. N., Hoa, N. T., Delgado, C., Chiou, S. K., Zhou, Y. H., and Judus, M. R. (2012) Differential glioma-associated tumor antigen expression profiles of human glioma cells grown in hypoxia. *PLoS ONE* **7**, e42661 [CrossRef Medline](#)
62. Breznik, B., Motaln, H., Vittori, M., Rotter, A., and Lah Turnšek, T. (2017) Mesenchymal stem cells differentially affect the invasion of distinct glioblastoma cell lines. *Oncotarget* **8**, 25482–25499 [CrossRef Medline](#)
63. Leloup, L., and Wells, A. (2011) Calpains as potential anti-cancer targets. *Expert Opin. Ther. Targets* **15**, 309–323 [CrossRef Medline](#)
64. Baudry, M., and Bi, X. (2016) Calpain-1 and Calpain-2: the yin and yang of synaptic plasticity and neurodegeneration. *Trends Neurosci.* **39**, 235–245 [CrossRef Medline](#)
65. Santos, D. M., Xavier, J. M., Morgado, A. L., Solá, S., and Rodrigues, C. M. (2012) Distinct regulatory functions of calpain 1 and 2 during neural stem cell self-renewal and differentiation. *PLoS ONE* **7**, e33468 [CrossRef Medline](#)
66. Godbout, R., Bisgrove, D. A., Shkolny, D., and Day, R. S., 3rd. (1998) Correlation of B-FABP and GFAP expression in malignant glioma. *Oncogene* **16**, 1955–1962 [CrossRef Medline](#)
67. Franken, N. A., Rodermond, H. M., Stap, J., Haveman, J., and van Bree, C. (2006) Clonogenic assay of cells *in vitro*. *Nat. Protoc.* **1**, 2315–2319 [CrossRef Medline](#)

A positive feedback loop involving nuclear factor IB and calpain 1 suppresses glioblastoma cell migration

The Minh Vo, Saket Jain, Rebecca Burchett, Elizabeth A. Monckton and Roseline Godbout

J. Biol. Chem. 2019, 294:12638-12654.

doi: 10.1074/jbc.RA119.008291 originally published online July 1, 2019

Access the most updated version of this article at doi: [10.1074/jbc.RA119.008291](https://doi.org/10.1074/jbc.RA119.008291)

Alerts:

- [When this article is cited](#)
- [When a correction for this article is posted](#)

[Click here](#) to choose from all of JBC's e-mail alerts

This article cites 66 references, 18 of which can be accessed free at <http://www.jbc.org/content/294/34/12638.full.html#ref-list-1>